Response to Referee #1's Comments

General Comments

Tang et al., have conducted a large scale and comprehensive campaign with the aim to explain key questions in the nature of long distance aerosol transport. The manuscript documents two major aspects of the aerosol samples: microscopy and molecular biology, through several sampling sites and spanning several dust events. The paper provided valuable findings relating an important process (Asian dust events) which may be applicable to many other similar systems worldwide.

Response: We thank the reviewer for his useful comments and suggestions. Those comments and suggestions helped us a lot to improve the quality of this paper. The authors have taken the comments from reviewers seriously and addressed all comments in current revision. Below are our point-by-point responses to those comments.

Specific Comments

Pg.1, Ln. 22 - I do not understand what "charge capacity" means throughout this paper. I can not find relevant results regarding "charge capacity" and microscopy. Did you mean something like fluorescence intensity, fluorescence concentration (as indicated when referring to some of the figures), or particle counts?

Response: The charge capacity means the ratios of the concentrations of two kinds of fluorescent particles. For example, the charge capacity of yellow fluorescent particles associated with the DAPI-stained bacteria means the ratios of the concentrations of DAPI-stained bacteria to those of yellow fluorescent particles. It can be referred to Figure 10 (a) and (b). In Figure 10, "[Fluorescent particle]/[Yellow particle]" means ratios of the concentrations of three kinds of fluorescent particles to those ('that' has been corrected) of the yellow particles. In order to avoid the reader's misunderstanding, '**the charge capacity**' has been replaced by '**the concentration ratios**' throughout the manuscript.

Original Text Pg.1 Ln.22: Moreover, the charge capacity of yellow fluorescent particles associated with the DAPI-stained bacteria increased from 5.1% ± 6.3% (non-dust samples) to 9.8% ± 6.3% (dust samples).

Amended Text Pg.1 Ln.22: Moreover, the concentration ratios of DAPI-stained bacteria to yellow fluorescent particles increased from 5.1% ± 6.3% (non-dust samples) to 9.8% ± 6.3% (dust samples).

Pg.5, Ln.7 - First mention of MiSeq should have company information (Illumina, CA, USA)

Response: By following the reviewer's suggestion, we have added '(Illumina, CA, USA)' when MiSeq is mentioned at the first time.

Pg.7, Ln.7 - in-text citation style should be "...previously described by Maki et al., (2014)." This should also be changed in other parts of the manuscript.

Response: By following the reviewer's suggestion, it has been corrected throughout the manuscript.

Pg.8, Ln.5 - Suggest changing to "phenol chloroform extraction/ethanol precipitation" for clarity.

Response: Thank the reviewer for helpful suggestions, we have modified it as you suggested.

Pg.8, Ln.6 - in-text citation style should be "Maki et al., (2017)"

Response: We thank the reviewer for the helpful suggestion, and have corrected it.

Pg.8, Ln.10 - Should include the hypervariable region(s) targeted (and the primer used) in the first step of PCR amplification.

Response: "During the first-step PCR amplification, fragments of 16S rDNA (which covers the variable region V4) were amplified from the extracted gDNA using the universal bacterial primers 515F (5'-Seq A-TGTGCCAGCMGCCGCGGTAA-3') and

806R (5'-Seq B-GGACTACHVGGGTWTCTAAT-3') (Caporaso et al., 2011), where Seq A and Seq B represent the nucleotide sequences bounded by the primer sets of second-step PCR. Detail process has been described by Maki et al. (2017)." has been added in '2.4 DNA extraction, sequencing and phylogenetic analysis'.

Pg.8, Ln.12 - This BioProject is not publicly available, it needs to be released.

Response: By following the reviewer's suggestion, the BioProject PRJNA413598 has been released on 2018-03-19.

Pg.9, Ln.16 - Consistency in period symbol: (Att. Bac. Coe.) (Dep. Rat.) (Col. Rat.)

Response: We thank the reviewer for helpful suggestion, the missing dots have been added throughout the manuscript.

Pg.14, Ln.4 - This seems to be a major observation/trend, why do you think this is the case?

Response: The major trend is "greater numbers of bacteria can be contained in a unit of yellow particles during dust events, whereas the black particles displayed the opposite behavior". Yellow particles (organic matter) can serve as nutrient sources for microbes, and favor their survival and long-distance transport. In addition, some dead microbes also emit yellow fluorescence. Therefore, it's reasonable that greater numbers of bacteria can be contained in a unit of yellow particles during dust events. On the contrary, more black particles (black carbon) was contained in a unit of yellow particles during non-dust events compared with dust events. Meanwhile, it is speculated that anthropogenic black carbon emission has a significant increase during non-dust periods comparing with that in dust events. It's worth noting that the mixing of the dust and black carbon during the long-distance transport (Fig. S4). Some researches show that the comparison of dust aerosols and anthropogenic pollutants (such as black carbon) shows a clear distinction of optical and radiative characteristics (Huang et al., 2011; Pu et al., 2015; Wang et al., 2010, 2013, 2014, 2015, 2017). Hence the further assessment of the radiative effects of the mixed-type aerosols is warranted.

Based on the above explanation, the manuscript has been revised as follows:

Original Text Pg.10 Ln.14: Under microscopic observation, the particles stained with DAPI emitted several types of fluorescence, mainly blue, white, yellow, or black fluorescence (Fig. 5). These particles were thus categorized as DAPI-stained bacteria (with diameters < 3 μm), white particles (mineral particles), yellow particles (organic matter) and black particles (black carbon) (Maki et al., 2017).

Amended Text Pg.10 Ln.14: Under microscopic observation, the particles stained with DAPI emitted several types of fluorescence, mainly blue, white, yellow, and black fluorescence (Fig. 5), which were thus categorized as DAPI-stained bacteria (with diameters < 3 μm), white particles (mineral particles), yellow particles (organic matter) and black particles (black carbon), respectively (Maki et al., 2017). There were a lot of yellow particles in dust samples, while black-particle concentrations increased in the samples collected in heavy air pollution days. The internal and external mixing between dust particles and black carbon were observed under the microscope (Fig. S4). Some researches show that dust aerosols and anthropogenic pollutant particles (black carbon) can be clearly distinguished in dependence on optical and radiative characteristics (Bi et al., 2016, 2017; Huang et al., 2011; Pu et al., 2015; Wang et al., 2014, 2015 and 2018). Hence the further assessment of the radiative effects of the mixed-type aerosols should be warranted.

Original Text Pg.13 Ln.1: It is speculated that the yellow particles (organic matter) and the white particles (mineral particles) serve as nutrient sources and shelters for microbes, respectively, and favor their survival and long-distance transport.

Amended Text Pg.13 Ln.1: It is speculated that the yellow particles (organic matter) and the white particles (mineral particles) serve as nutrient and shelters for microbes, respectively, and favor their survival and long-distance transport. Some dead cells and debris of microbes are thought to also emit yellow fluorescence (Liu et al., 2014).

Original Text Pg.13 Ln.11: The ratio of the concentrations of the DAPI-stained bacteria, the black particles and the white particles to those of the yellow particles were

considered together with the charge capacity of the yellow particles. The charge capacity of the yellow particles for the DAPI-stained bacteria increased slightly with the concentrations of the yellow particles (Fig. 10a). This result indicates that the yellow particles (organic matter) in the dust may serve as nutrient sources and favor microbial survival, which is also partly confirmed by the micrographs (Fig. 6a, b, c and d). The ratios of the concentrations of the DAPI-stained bacteria, the black particles and the white particles to those of the yellow particles ranged from 5.1% ± 6.3% (non-dust samples) to 9.8% ± 6.3% (dust samples), from 73.6% ± 100.4% (non-dust samples) to 9.0% ± 8.2% (dust samples), and from 2.7% ± 3.3% (non-dust samples) to 3.8% ± 4.1% (dust samples), respectively (Fig. 10b). It is quite clear that the charge capacity of the yellow particles associated with the DAPI-stained bacteria was higher in the dust samples compared with that in the non-dust samples. On the other hand, the charge capacity of the yellow particles associated with the black particles was much lower in the dust samples; thus, greater numbers of bacteria can be contained in a unit of yellow particles during dust events, whereas the black particles displayed the opposite behavior.

Amended Text Pg.13 Ln.11: The concentration ratios of the DAPI-stained bacteria, the black particles and the white particles to the yellow particles were calculated (Fig. 10). The concentration ratios of the DAPI-stained bacteria, the black particles and the white particles to the yellow particles ranged from 5.1% ± 6.3% (non-dust samples) to 9.8% ± 6.3% (dust samples), from 73.6% ± 100.4% (non-dust samples) to 9.0% ± 8.2% (dust samples), and from 2.7% ± 3.3% (non-dust samples) to 3.8% ± 4.1% (dust samples), respectively (Fig. 10b). The concentration ratios of the DAPI-stained bacteria to the yellow particles were much higher in the dust samples than in the non-dust samples, while the concentration ratios of the black particles to the yellow particles significantly decreased in the dust samples in comparison to the non-dust samples. Thus, greater numbers of bacteria can be contained in a unit of yellow particles during dust events, whereas the black particles displayed the opposite behavior. The results indicate that the yellow particles (organic matter) in the dust may serve as nutrient and favor microbial survival and long-distance transport, which was also partly confirmed by the micrographs (Fig. 6a, b, c and d). In contrast, anthropogenic black carbon load in the

dust samples decreased significantly comparing to non-dust samples.

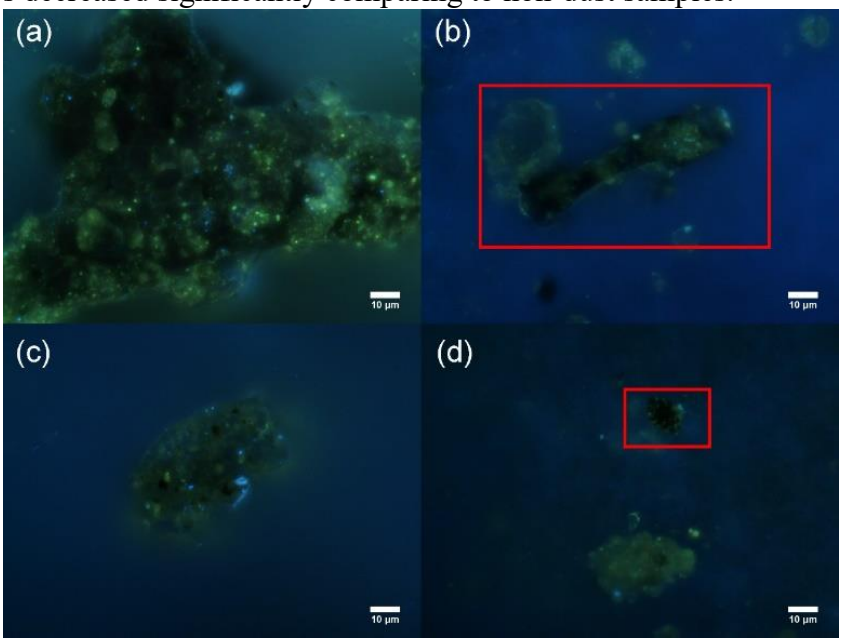

Fig. S4 Epifluorescence micrograph of mixed-type aerosols, (a) from the sample ER4_15D2, (b) and (d) from the sample ER4_11N, (c) from the sample ER4_15N1.

Pg.14, Ln.6 - For reproducibility, please consider uploading the OTU sequences as supplemental files in FASTA format.

Response: By following the reviewer's suggestion, all 16S OTU sequence data has been uploaded in FASTA format.

Pg.15, Ln.21 - Avoid contraction, use "It is"

Response: By following the reviewer's suggestion, we have corrected.

Pg.17, Ln.9 - Avoid contraction, use "It is"

Response: We thank the reviewer for helpful suggestions again, and have corrected it.

Response to Referee #2's Comments

General Comments

Bioaerosols are a class of atmospheric particles, which are more likely to participate in long-distance transport and be observed in other regions. This manuscript investigated the effects of dust events originating in the Gobi Desert of Asia on the amount and diversity of bioaerosols. In this study, sufficient and comprehensive experimental data was presented to reveal that the number of bacteria and the diversity of the bacterial communities showed remarkable increases during the dust events. Microscopic observations made with DAPI staining and MiSeq sequencing analysis were used to determine the results. In general, this manuscript was well-organized and the main conclusions will help improve the current understanding of bioaerosol dynamics along the transport pathway of Asian dust in China. This manuscript should be published in ACP after a little more discussion and analysis to clarify the details behind the presented results.

Response: We would like to thank the reviewer for his positive comments and suggestions. Those comments and suggestions helped us a lot to improve the quality of this paper. The authors have taken the comments from reviewers seriously and addressed all comments in current revision. Below are our point-by-point responses to those comments.

Specific Comments

Page 5 line 3. The result of Jinan samples should be compared with the result from another bioaerosol campaign (AAQR 18, 1-14, 2018).

Response: We thank the reviewer for helpful suggestions, it is of great importance to explore the difference of the bacterial communities between air samples (or dust samples) and cloud samples (Zhu et al., 2018). In this manuscript, 22 samples from Erenhot (17 samples) and Mongolia (5 samples) were analysed by MiSeq sequencing, while Jinan samples were not yet analysed. In spite of this, the comparison between

these 22 samples and cloud samples should be inspirational. In the cloud samples of Mt. Tai (Zhu et al., 2018), the dominant bacterial phylum was *Firmicutes*, whose averaged relative abundance was 80.5%, and *Proteobacteria*, *Bacteroidetes*, *Actinobacteria*, and *Fusobacteria* were the following. While *Bacteroidetes* and *Proteobacteria* were the dominant in these 22 air samples, followed by *Actinobacteria* (Fig. 14). The relative abundance of *Firmicutes* did not exceed 5%, and the phylum *Fusobacteria* was not found in these 22 air samples (Fig. S4).

Original Text Pg.16 Ln.15-19 was deleted: At the class level, *Chloracidobacteria* and *Gemmatimonadetes* in dust samples of Erenhot and non-dust samples of R-DzToUb have higher relative amounts compared with non-dust samples of Erenhot and dust samples of R-DzToUb (Fig. 15). *Cytophagia* in the phylum *Bacteroidetes* shows similar phenomenon. Further, *Bacilli* in non-dust samples of Erenhot shows very low amounts down to the detection limit, whereas its relative amounts in other samples keep stable.

Original Text Pg.17 Ln.7: Furthermore, *Firmicutes* was the predominant phylum in the Gobi Desert. The proportions of this phylum reach as high as 82% in surface sand samples, but it was found in relatively small proportions that did not exceed 5% in the air samples (Fig. 14). It's clear that the bacterial community composition in the air is very different from that in the surface sand or soil.

Amended Text Pg.17 Ln.7: The relative abundance of *Firmicutes* increased slightly in the dust samples compared with the non-dust samples (Fig. 14). *Firmicutes* was the predominant phylum of surface sand samples in the Gobi Desert of Asia, but not in the Taklamaken Desert (An et al., 2013). The relative abundance of *Firmicutes* could reach as high as 82% in the surface sand samples from the Gobi Desert of Asia (44.3°N, 110.1°E) (An et al., 2013), but it was found in relatively small proportions that did not exceed 5% in all the air samples (Fig. 14). Maki et al. (2016) found that the relative

abundance of *Firmicutes* in air samples from the Gobi Desert of Asia (44.2304°N, 105.1700°E) varied greatly, from 15.7 to 40.5% in non-dust samples, and no more than 12% in dust samples. The sequences of *Firmicutes* mainly belonged to the classes *Bacilli* and *Clostridia* in air samples from Tsogt-Ovoo, Mongolia (Maki et al., 2016). While *Bacilli*, *Clostridia* and *Erysipelotrichi* in the phylum *Firmicutes* were found in the air samples from Erenhot (Fig. S5). The averaged relative abundance of *Bacilli* in dust samples from Erenhot was 3.2%, while it is much lower in non-dust samples (Fig. 15). It is worth mentioning that Zhu et al. (2018) found that the averaged relative abundance of *Firmicutes* in cloud samples at Mt. Tai of China was 80.5%. As for the Taklimakan Desert, Puspitasari et al. (2015) analyzed the bacterial diversity in sand dunes and dust aerosol, and the relative abundance of *Firmicutes* in dust aerosol samples was higher than that in surface sand samples, which shows a different pattern comparing to the Gobi Desert of Asia. In conclusion, the bacterial community compositions in the air are different from that in the surface sand or soil, and differ by the location and transmitting vector.

Page 9, line 20 – page 10 line 4. The concentrations of PM2.5 increased significantly in Zhangbei during D2, D3 and D7. It seems that Zhangbei was seriously affected by the dust events in Erenhot. But the next part of the paper said that Zhangbei was slightly affected by the dust events based on D6. The authors need to explain it.

Response: During the dust event 'D6', the PM2.5 mass concentrations showed a slight increase, not as heavy as D2, D3 and D7. In addition, the barometric pressure of D6 was relatively stable, but that of D2, D3 and D7 were on the contrary, showing a significant decrease. Thereby, Zhangbei was slightly affected by the dust events during the dust event 'D6'.

Original Text Pg.10 Ln.2: A slight increase in $PM_{2.5}$ mass concentrations was observed during event D6, accompanied by a strong north wind, indicating that Zhangbei was slightly affected by the dust events that occur in Erenhot.

Amended Text Pg.10 Ln.2: A slight increase in $PM_{2.5}$ mass concentrations was observed during the event D6, accompanied by a strong north wind and the relatively

stable atmospheric pressure, indicating that Zhangbei was slightly affected by the dust event that occurred in Erenhot at that time.

Page10 line 19. The name of the sample should be ER4_12D. Please be sure that all the samples' names are correct.

Response: By following the reviewer's suggestion, we have corrected it throughout the manuscript.

Page14 line6. The analyzed 22 samples were collected in Erenhot or Zhangbei?

Response: The analyzed 22 samples were collected in Erenhot and on the road between Dalanzadgad and Ulaanbaatar (R-DzToUb). The names of the 22 samples can be referred to x-coordinate label of Fig. 11. And detailed sample information can be referred to Table S1 and Table S3.

In Fig. 4. Please clarify the meaning of different colors of the air masses.

Response: The different colors of the trajectories mean the different backward trajectory ending time. The trajectory with red color is the backward trajectory which has the latest ending time. Blue is the next, then green, cyan, purple, yellow.

In Fig.9 and in Fig. 10(a). How the authors get the fitting curves and fitting areas. Please clarify it.

Response: The fitting curves and fitting areas were plotted by R software, and the function stat_smooth (method=lm, level=0.95) in the package 'ggplot2' was used. The fitting curves were calculated by the linear regression method, and the independent variable was sorted before regression. The fitting areas were calculated based on the confidence interval of 95%.

Response to Referee #3's Comments

General Comments

This paper examines atmospheric bioaerosols at three sites downwind of the Gobi Desert in the Dust-Bioaerosol 2016. The authors found that the number of bacteria and the diversity of the bacterial communities increased significantly during the dust events by microscopic observations made with DAPI staining and MiSeq sequencing analysis. In general, this is a well-written paper that presents interesting data. It will be of interest to readers of this Journal, particularly researchers in the field.

Response: We sincerely thank the reviewer for his suggestions. Those suggestions helped to improve the quality of this paper. The authors have taken the comments from reviewer seriously and addressed all comments in current revision. Below are our point-by-point responses to those comments.

Specific Comments

Page 2, line 6: "proteobacteria" should be capitalized.

Response: By following the reviewer's suggestion, we have corrected it.

Page 8: The description of the methods of MiSeq sequencing should be limited. It would help readers if the authors gave a more detailed explanation.

Response: We thank the reviewer for the helpful suggestion, and have revised section 2.4 as follow.

Original Text Pg.8 Ln.4: The genomic DNA (gDNA) was extracted from the atmospheric samples from Erenhot and Mongolia using the PC extraction/alcohol precipitation method. Two-step PCR amplification and product purification were then carried out according to the method of Maki (Maki et al., 2017). Two-step PCR has several advantages, such as increased reproducibility and the recovery of greater levels of genetic diversity during amplicon sequencing (Park et al., 2016). An Illumina MiSeq sequencing system (Illumina, CA, USA) and a MiSeq Reagent Kit V2 (Illumina, CA,

USA) were used to perform the sequencing, and an average read length of 270 bp was obtained. All the data obtained from MiSeq sequencing have been deposited in the DDBJ/EMBL/GenBank database, and the accession number of the submission is PRJNA413598.

Amended Text Pg.8 Ln.4: The genomic DNA (gDNA) was extracted from the atmospheric samples from Erenhot and Mongolia using the phenol chloroform extraction/ethanol precipitation method (Maki et al., 2017). Two-step PCR amplification and product purification were then carried out according to the method of Maki et al. (2017). Two-step PCR has several advantages, such as increased reproducibility and the recovery of greater levels of genetic diversity during amplicon sequencing (Park et al., 2016). During the first-step PCR amplification, fragments of 16S rDNA (which covers the variable region V4) were amplified from the extracted gDNA using the universal bacterial primers 515F (5'-Seq A-TGTGCCAGCMGCCGCGGTAA-3') and 806R (5'-Seq B-GGACTACHVGGGTWTCTAAT-3') (Caporaso et al., 2011), where Seq A and Seq B represent the nucleotide sequences bounded by the primer sets of second-step PCR. Detail process has been described by Maki et al. (2017). An Illumina MiSeq sequencing system (Illumina, CA, USA) and a MiSeq Reagent Kit V2 (Illumina, CA, USA) were used to perform the sequencing, and an average read length of 270 bp was obtained. All the data obtained from MiSeq sequencing have been deposited in the DDBJ/EMBL/GenBank database, and the accession number of the submission is PRJNA413598.

Page 10, line 18 to Page 11, lines 8, Fig. 6, and Table S1: The sample names contain a

number of errors. Please check all sample names, including sampling information, and revise them accordingly.

Response: We thank the reviewer for the helpful suggestion, and have corrected all sample names throughout the manuscript and checked the sampling information in the supplement. In Pg.10 Ln.19, the sample name 'ER4_12' has been corrected to 'ER4_12D'.

Page 14, lines 11 and 14: "orders (and class level candidate taxa)" should be "orders (and order-level candidate taxa)".

Response: By following the reviewer's suggestion, we have corrected it.

Fig. 9: The authors should check the symbols in Fig. 9. "DAPI-stained bacteria" should be "Black particle" in Fig. 9 (a). In contrast, "Black particle" should be "DAPI-stained bacteria" in Fig. 9 (b).

Response: We thank the reviewer for the helpful suggestion, and have corrected the symbols in Fig. 9.

Characterization of atmospheric bioaerosols along the transport pathway of Asian dust during the Dust-Bioaerosol 2016 Campaign

Kai Tang[1], Zhongwei Huang[1*], Jianping Huang[1], Teruya Maki[2], Shuang Zhang[1], Atsushi Shimizu[3], Xiaojun Ma[1], Jinsen Shi[1], Jianrong Bi[1], Tian Zhou[1], Guoyin Wang[1], Lei Zhang[1]

[1]Key Laboratory for Semi-Arid Climate Change of the Ministry of Education, College of Atmospheric Sciences, Lanzhou University, Lanzhou, 730000, China.
[2]College of Science and Engineering, Kanazawa University, Kakuma, 920-1192, Japan
[3]National Institute for Environmental Studies, Tsukuba, ~~Ibaraki~~, 305-8506, Japan

Correspondence to: Zhongwei Huang (huangzhongwei@lzu.edu.cn)

Abstract

Previous studies have shown that bioaerosols are injected into the atmosphere during dust events. These bioaerosols may affect leeward ecosystems, human health and agricultural productivity and may even induce climate change. However, bioaerosol dynamics have rarely been investigated along the transport pathway of Asian dust, especially in China, where dust events affect huge areas and massive numbers of people. Given this situation, the Dust-Bioaerosol (DuBi) Campaign was carried out over northern China, and the effects of dust events on the amount and diversity of bioaerosols were investigated. The results indicate that the number of bacteria showed remarkable increases during the dust events, and the diversity of the bacterial communities also increased significantly, as determined by means of microscopic observations with 4,6-diamidino-2-phenylindole (DAPI) staining and MiSeq sequencing analysis. These results indicate that dust clouds can carry many bacteria of various types into downwind regions and may have potentially important impacts on ecological environments and climate change. The abundances of DAPI-stained bacteria in the dust samples were one to two orders of magnitude greater than those in the non-dust samples and reached 10^5 ~ 10^6 particles·m^{-3}. Moreover, the concentration ratios ~~charge capacity~~ of DAPI-stained bacteria to yellow fluorescent particles ~~associated~~

带格式的: 上标

带格式的: 字体: (中文) Times New Roman, 上标

带格式的: 字体: (中文) Times New Roman

带格式的: 字体: (中文) Times New Roman

~~with the DAPI-stained bacteria~~ increased from 5.1% ± 6.3% (non-dust samples) to 9.8% ± 6.3% (dust samples). A beta diversity analysis of the bacterial communities demonstrated the distinct clustering of separate prokaryotic communities in the dust and non-dust samples. *Actinobacteria*, *Bacteroidetes*, *Proteobacteria* remained the dominant phyla in all samples. As for Erenhot, the relative abundances ~~amounts~~ of *Acidobacteria* and *Chloroflexi* ~~have~~ had a remarkable rise in dust events. On the contrary, the relative abundances of *Acidobacteria* and *Chloroflexi* in non-dust samples of R-DzToUb were greater than those in dust samples. *Alphaproteobacteria* made the major contribution of the increasing relative abundance ~~amounts~~ of the phylum *Pp~~p~~roteobacteria* in all dust samples. The relative abundance of *Firmicutes* did not exceed 5% in all the air samples, even though it is the predominant phylum in the surface sand samples in the Gobi Desert of Asia. These results illustrate that the bacterial community contained in dust aerosol samples have a different pattern compared with non-dust aerosol samples, and the relative abundances of airborne bacteria are different from those in the surface sand or soil, and differ by the location and transmitting vector. ~~In the future, the viability and activity of airborne microbes, the interactions between bioaerosols and other gaseous and solid components in the air, and the effects of bioaerosols on animals and plants, ecological environments and the climate system must be studied in depth to help us understand the behavior of bioaerosols in the air and dust clouds in greater detail.~~

1 Introduction

Bioaerosols are a class of atmospheric particles that range in size from nanometers up to about a tenth of a millimeter. They are made up of living and dead organisms (e.g., algae, archaea, and bacteria),

dispersal units (e.g., fungal spores and plant pollen), and various fragments or excretions (e.g., plant debris and brochosomes) (Fröhlich-Nowoisky et al., 2016). Several studies have investigated the role of dust events as a vehicle for bioaerosols (Hervàs et al., 2009; Prospero et al., 2005; Sugimoto et al., 2012; Yamaguchi et al., 2012). Asian dust events are capable of moving masses of soil-derived dust over long distances and may introduce large amounts of microorganisms and pollen to the atmosphere. It is well known that Asian dust frequently disperses all around the East Asian regions (Iwasaka et al., 1983; Huang et al., 2008a; Huang et al., 2010) and can even reach the Americas (Husar et al., 2001) and the Arctic (Huang et al., 2015). Asian dust clouds can sometimes be transported more than one full circuit around the globe in approximately 13 days (Uno et al., 2009), and Asian dust has been identified in ice and snow cores from Greenland (Bory et al., 2003) and the French Alps (Grousset et al., 2003). Drylands are one of the most sensitive areas to climate change and human activities, and the increasing aridity, enhanced warming and rapidly growing human population will exacerbate the risk of land degradation and desertification in the near future in the drylands (Huang et al., 2015, 2017a~~, 2017~~b). ~~Climate change (Prospero and Lamb, 2003) and anthropogenic causes (Neff et al., 2008) may increase the magnitude and frequency of dust storms in semi-arid and arid regions in the near future.~~

Increasing evidence shows that microbes are transported by Asian dust events (Hua et al., 2007; Maki et al., 2017; Yeo and Kim, 2002). In Japan, the concentrations of bacterial cells and the structure of airborne bacterial communities in the near-surface air and the free troposphere are affected by Asian dust events (Maki et al., 2014, 2015). Similarly, the yellow sandstorms that originate in Asian deserts have been reported to affect the ambient air quality of Taiwan by increasing the levels of fungal spores

(Ho et al., 2005; Wu et al., 2004). Results from South Korea also show that Asian dust impacts both airborne fungal concentrations and fungal communities (Jeon et al., 2011, 2013; Yeo and Kim, 2002).

Considering the transoceanic and transcontinental dispersal of bioaerosols associated with dust events, the importance of bioaerosols in the atmosphere is likely to be seriously underestimated. These bioaerosols may affect leeward ecosystems, human health, and agricultural productivity, and they may play a larger role in the climate system by acting as efficient ice nucleating particles and cloud condensation nuclei. Certain species of bacteria and fungi are known to have very high ice nucleating (IN) ability, especially at warmer temperatures (Maki and Willoughby, 1978), potentially leading to the initiation of ice formation in clouds and thereby influencing precipitation, cloud dynamics and the amount of incoming and outgoing solar radiation (Creamean et al., 2013). A study used a cloud simulation chamber to demonstrate that bacterial IN activity is maintained even after cell death (Amato et al., 2015). Hence, the role of microorganisms in the atmosphere is an underappreciated aspect of biological and atmospheric science; these microorganisms have potentially important impacts on the hydrological cycle, clouds, and climate (DeLeon-Rodriguez et al., 2013).

Moreover, bioaerosols may have a significant influence on human health and the spread of plant diseases. Airborne microorganisms containing bacteria, fungi and viruses can have infectious, allergenic, or toxic effects on living organisms, causing disease or allergies in humans, agricultural crops, livestock, and ecosystems, including coral reefs. The dust event-driven dispersal of bioaerosols is strongly correlated with allergen burdens and asthma (Griffin, 2007; Ichinose et al., 2005; Liu et al., 2014). The long-distance aerial dispersal of pathogens by the wind can spread plant diseases (Brown and

Hovmøller, 2002) and human diseases, such as Kawasaki disease (Jorquera et al., 2015; Rodo et al., 2011).

Therefore, information on the abundance of bioaerosols in the ~~this~~ dust is necessary to assess the influence of these bioaerosols on public health, ecosystems, biogeographical distributions, and meteorological and climatic processes (Hara and Zhang, 2012). Recent research has showed that the Gobi Desert of Asia, instead of the Taklimakan Desert, plays the most important role in contributing to dust concentrations in East Asia, and approximately 35% of the dust emitted from the Gobi Desert of Asia is transported to remote areas in East Asia in spring (Chen et al., 2017). To investigate the effects of dust events from the Gobi Desert of Asia on the amount and diversity of microbes in the air, the Dust-Bioaerosols (DuBi) Campaign was carried out during March through May in 2016. This campaign is named "DuBi-2016" in this paper (Fig. 1).

In the DuBi-2016 campaign, air sampling was performed continuously at three sites downwind of the Gobi Desert of Asia. These sites lie along the transport path of Asian dust, which were Erenhot, Zhangbei and Jinan. Frequent dust storms attacked Erenhot directly, and a great amount of transported dusts were ~~was~~ observed there. Only a small number of them, by contrast, could arrive in Zhangbei and Jinan. In addition, some samples were collected on the road between Dalanzadgad and Ulaanbaatar, and these samples enable comparison of the structure of microbial communities between the source and downwind regions. Through combining microscopy and MiSeq sequencing analysis (Illumina, CA, USA), the potential effects of long-range transported dust on the amount and diversity of bioaerosols can be well characterized.

2 Experiments

2.1 Sample collection

Information on the sampling sites is provided in Table 1. The sampling sites in Erenhot and Zhangbei ~~are~~ were located to the northwest of the residential area and at a distance from this area. Anthropogenic activities that might influence the sites ~~are~~ were not expected in cases in which air masses arrive from the south, southwest, west, or northwest. Therefore, the dust particles appearing at the sites had traveled long distances in the atmosphere and originated primarily in Mongolia and northern China. In addition, five bioaerosol samples were collected on the car along the road between Dalanzadgad and Ulaanbaatar (R-DzToUb). These samples represent conditions in the dust source regions.

The bioaerosol samples were collected using four sterilized polycarbonate filters with a pore size of 0.2 μm (Whatman, 111106, China) with a sterilized Swinnex 13-mm filter holder (Millipore, SX0001300, China) connected to an air pump (AS ONE, MAS-1, Japan; the flow rate for each filter was approximately 0.3 $L \cdot min^{-1}$) for 1~24 h, according to air quality conditions. Whenever dust arrived, intensive observations were made to get the information on the fine structure of the dust event. Before sampling, all ~~of~~ the filters were sterilized by autoclaving (121°C for 20 min). After sampling, the samples were stored at -80 °C until the downstream analyses were performed.

To avoid contamination, the sampling filter holders and the materials used to change the filters were treated with 75% ethanol every day, and a mask was worn during operation. Detailed information on the samples is provided in Table S1, Table S2, and Table S3.

2.2 Meteorological data and aerosol information

In Erenhot, a ~~TR-74Ui~~ device (T&D Corporation, TR-74Ui, Japan) was used to measure the temperature, relative humidity, illuminance and UV intensity sequentially. Data describing the attenuated backscatter coefficient, the volume depolarization ratio, and the color ratio were obtained from ~~the~~ Zamynuud observation site of AD-Net (43.72° N, 111.90° E, 962 m ASL), which is located less than 10 km away from the sampling site in Erenhot (Nishizawa et al., 2016; Shimizu et al., 2016).

In Zhangbei, basic meteorological information, including measurements of temperature, relative humidity, pressure, wind, precipitation and radiation, was gathered by an automatic meteorological station (weather transmitter WXT520, Vaisala), and the $PM_{2.5}$ mass concentrations were measured using a continuous ambient particulate TEOM™ ~~M~~monitor (Series 1400a, Thermo Fisher Scientific Inc.) (~~Bi et al., 2017; Jianping and Xin~~Huang et al., 2008b; Wang et al., 2010).

Seventy-two-hour backward trajectories of the air masses at the Zhangbei observational site were calculated using the National Oceanic and Atmospheric Administration Hybrid Single Particle Lagrangian Integrated Trajectory (HYSPLIT) model (http://www.arl.noaa.gov/HYSPLIT.php).

2.3 Sample analysis

The total number of microorganisms in the bioaerosols was determined by a modified counting method that was previously described by ~~Maki (~~Maki et al.~~,~~ (2014). The samples were stained with 10 $\mu g \cdot mL^{-1}$ 4,6-diamidino-2-phenylindole (DAPI, ~~;~~ D9542, Sigma, China; the DAPI-DNA complex has an excitation wavelength of 364 nm and an emission wavelength of 454 nm) for 15 min after being fixed in a 4% paraformaldehyde solution for 1 h. The filter was then placed on a slide in a drop of low-fluorescence immersion oil (IMMOIL-F30CC, Olympus). A second drop of oil was added, and a

coverslip was placed on top. Next, the prepared slides were observed using an epifluorescence microscope (BX53 and DP72, Olympus, Japan) equipped with an ultraviolet excitation system; an excitation waveband of 340~390 nm was used. Fluorescent particles with four different colors, blue, white, yellow, and black, were counted in 10 randomly selected fields. The fluorescent particle concentrations in the bioaerosols were calculated using the following formula:

$$C = \frac{S_1 \times N_0}{S_0 \times V}, \quad (1)$$

where C is the number of fluorescent particles in the bioaerosols (particles·m^{-3}), S_1 is filtration area on the membrane (7×10^7 μm^2), S_0 is the area of each microscopic field (1.46×10^4 μm^2), N_0 is the average number of fluorescent particles in the microscopic field, and V is the volume of the filtered sample (m^3). The detection limit of the particles is approximately 1.0×10^4 particles m^{-3} of air.

2.4 DNA extraction, sequencing and phylogenetic analysis

The genomic DNA (gDNA) was extracted from the atmospheric samples from Erenhot and Mongolia using the phenol chloroform extraction/ethanol precipitation ~~the PC extraction/alcohol precipitation~~ method (Maki et al., 2017). Two-step PCR amplification and product purification were then carried out according to the method of ~~Maki (~~Maki et al.~~,~~ (2017). Two-step PCR has several advantages, such as increased reproducibility and the recovery of greater levels of genetic diversity during amplicon sequencing (Park et al., 2016). During the first-step PCR amplification, fragments of 16S rDNA (which covers the variable region V4) were amplified from the extracted gDNA using the universal bacterial primers 515F (5'-Seq A-TGTGCCAGCMGCCGCGGTAA-3') and 806R (5'-Seq B-GGACTACHVGGGTWTCTAAT-3') (Caporaso et al., 2011), where Seq A and Seq B represent the

nucleotide sequences bounded by the primer sets of second-step PCR. Detail process has been described by Maki et al. (2017). An Illumina MiSeq sequencing system (Illumina, CA, USA) and a MiSeq Reagent Kit V2 (Illumina, CA, USA) were used to perform the sequencing, and an average read length of 270 bp was obtained. All the data obtained from MiSeq sequencing have been deposited in the DDBJ/EMBL/GenBank database, and the accession number of the submission is PRJNA413598.

The R software package (version 3.4.1) was employed to analyze the experimental data. The "phyloseq" package (version 1.20.0) was used to handle and analyze the high-throughput sequencing data. The Shannon index (H′) and the Simpson index (D) are calculated as follows:

$$H' = -\sum_{i=1}^{S} P_i * log_2 P_i, \quad (2)$$

$$D = 1 - \sum_{i=1}^{S} (P_i)^2, \quad (3)$$

where S is the number of operational taxonomic units (OTUs), and P_i is the relative proportion of an individual species i.

Principal coordinate analysis (PCoA) with weighted UniFrac distances was used to explore and visualize similarities or dissimilarities of the bacterial communities contained in samples. UniFrac measures the difference between two collections of sequences as the amount of evolutionary history that is unique to either of the two, which is measured as the fraction of branch length in a phylogenetic tree that leads to descendents of one sample or the other but not both (Lozupone et al., 2011). There are two phylogenetic measures of community β diversity: unweighted UniFrac, a qualitative measure, which use only the presence/absence of data, and weighted UniFrac, a quantitative measure, which use the abundance of each taxon (Lozupone et al., 2007). UniFrac, coupled with standard multivariate statistical

techniques including principal coordinates analysis (PCoA) can be used to cluster many samples according to the difference of their bacterial communities.

3 Results and discussion

3.1 Identification of the dust events

The dust events in spring 2016 were identified from lidar observations ~~made~~ in Zamynuud and $PM_{2.5}$ mass concentrations ~~measured~~ in Zhangbei. In addition, meteorological factors, such as atmospheric pressure, wind speeds and wind directions, were checked to confirm the dust events in Zhangbei. Polarization measurements from lidar remote sensing is very useful to identify the dust events from others (Zhou et al., 2013; Sugimoto and Huang, 2014). The attenuated backscattering coefficient at 532 nm (Att. Bac. Coe.), the volume depolarization ratio (Dep. Rat.) and the color ratio (Col. Rat.) increased dramatically when the dust events occurred. Seven heavy dust events (D1-D7) occurred in Erenhot during the sampling period (Fig. 2). Accordingly, the samples collected during the events D1-D7 were ~~are~~ named ~~the~~ "dust samples" (Table S1). During the events D2, D3 and D7, the mass concentrations of $PM_{2.5}$ in Zhangbei increased significantly with northwest or north winds, increasing wind speed and an apparent decline of atmospheric pressure (Fig. 3). These observations indicate that dust events occurred in Zhangbei at that time. A slight increase in $PM_{2.5}$ mass concentrations was observed during the event D6, accompanied by a strong north wind and the relatively stable atmospheric pressure, indicating that Zhangbei was slightly affected by the dust event~~s~~ that occurred in Erenhot at that time. Accordingly, the samples ZB3_31N, ZB4_6D, ZB4_6N, ZB4_21D were considered as "dust samples" (Table S2). The 72-h back trajectories of air masses in

Zhangbei calculated using the HYSPLIT model indicate that the dust events D2, D3, D6 and D7 originated in the Gobi Desert of Asia and passed over Erenhot and Zhangbei during the transport process. Several peaks in $PM_{2.5}$ concentrations appeared in Zhangbei on Mar. 30, Apr. 4 and Apr. 11. These peaks were not dust events, as determined using the wind speeds, wind directions and 72-h back trajectories (Figs. 3 and 4). An air pollution event named "P1" occurred on Apr. 11 that was characterized by high $PM_{2.5}$ concentrations, strong south winds and air masses that originated in the southern regions (Fig. 4).

3.2 State of the bioaerosols in the dust and non-dust samples

~~Under microscopic observation, the particles stained with DAPI emitted several types of fluorescence, mainly blue, white, yellow, or black fluorescence (Fig. 5). These particles were thus categorized as DAPI-stained bacteria (with diameters < 3 μm), white particles (mineral particles), yellow particles (organic matter) and black particles (black carbon) (Maki et al., 2017).~~

Under microscopic observation, the particles stained with DAPI emitted several types of fluorescence, mainly blue, white, yellow, and black fluorescence (Fig. 5), which were thus categorized as DAPI-stained bacteria (with diameters < 3 μm), white particles (mineral particles), yellow particles (organic matter) and black particles (black carbon), respectively (Maki et al., 2017). There were a lot of yellow particles in dust samples, while black-particle concentrations increased in the samples collected in heavy air pollution days. The internal and external mixing between dust particles and black carbon were observed under the microscope (Fig. S4). Some researches show that dust aerosols and anthropogenic pollutant particles (black carbon) can be clearly distinguished in dependence on optical and radiative characteristics (Bi et al., 2016, 2017; Huang et al., 2011; Pu et al., 2015; Wang et al., 2014,

2015 and 2018). Hence the further assessment of the radiative effects of the mixed-type aerosols should be warranted.

Analysis of the microphotographs shows that the dust and non-dust samples were significantly different. As two examples, ER4_12D was compared with ER4_13, and ER4_15D1 was compared with ER4_16. Compared with the sample ER4_16, which was collected during a non-dust event, the dust sample ER4_15D1 contained a surprising number of DAPI-stained bacteria (coccoid- or bacillus-like bacteria) (Fig. 6a and b). This comparison clearly demonstrates that dust events can carry large amounts of bacteria into the atmosphere, and these microbes continue to float towards downwind regions. We also take the dust events that occurred on Apr. 12 and 13 as another example. These events differed somewhat from each other in terms of their dust intensity and dust blowing height. The lidar data clearly demonstrate that the dust mass noted on Apr. 12 fell to the ground from nearly 4 km, whereas the dust event that occurred on Apr. 13 was mild by contrast and likely originated from a local source. The sample ER4_12D contained more DAPI-stained bacteria, although the sampling duration was shorter than that of the sample ER4_13 (Fig. 6c and d). This result illustrates that dust transported over long distances containeds large amounts of microorganisms and may have substantial impacts on downwind regions. In addition, epifluorescence microscopy has revealed that aerosols collected at 800 m over the Taklimakan Desert contained large particles attached with microorganisms, such as bacteria (Maki et al., 2008). Airborne microbes are often attached to larger particles especially yellow particles and found as agglomerates (Tong and Lighthart, 2000), which may help them survive nutrient shortages and UV radiation and may even facilitate the growth and reproduction of the microbes.

Under the SEM, the bioaerosols ~~were seen to~~ displayed various states (Fig. 7). Spiny fungal spores (Fig. 7a) and shriveled pollen (Fig. 7d) may represent strategies that organisms take to protect themselves from the harsh atmospheric environment and ensure their survival. Entering a non-dividing state (dormancy) in which they transform morphologically to spores or undergo other cell wall modifications and slow down or stop their metabolic activity can improve their resistance to physical stresses, such as desiccation and UV radiation, which increases their chances of survival in the atmosphere (Smets et al., 2016). Furthermore, some coccus-like airborne microbes were found attached to mineral particles (Fig. 7e and f), which may serve as shelters and favor the survival of the bacteria. Interestingly, exocytosis or endocytosis (Fig. 7c) and cell division processes (Fig. 7b) were captured, showing that microbial activity proceeds in the air.

3.3 Variations in the concentrations of fluorescent particles in the dust and non-dust samples

When the Asian dust events occurred in downwind area, airborne microbial abundances increased at 10- or 100-folds (Hara and Zhang, 2012), and showed relative correlation with PM_{10}, which are indicators of dust occurrences (Dong et al., 2016, Cha et al., 2016 and 2017). In this study, the concentrations of the DAPI-stained bacteria, the white particles and the yellow particles in the dust samples were significantly higher than those in the non-dust samples, whereas the concentrations of the black particles (black carbon) showed no obvious pattern, regardless of the occurrence of dust events (Fig. 8a, b and c). In general, the concentrations of DAPI-stained bacteria in the non-dust samples were on the order of 10^4 to 10^5 particles·m^{-3}, whereas those in the dust samples were 10^5 to 10^6 particles·m^{-3}. These concentrations are similar to the results of other field observations made in Tsogt-Ovoo in the Gobi Desert of Asia (Maki et al., 2016) and indicate that dust events can carry abundant microbes. In

addition, the concentrations of the yellow particles in the non-dust and dust samples were on the order of 10^5 to 10^6 particles·m^{-3} and 10^6 to 10^7 particles·m^{-3}, respectively. Aerosols transported by Asian dust events are reported to include high amounts of organic molecules, such as mannitol, glucose, and fructose, which consist of the cell components of airborne microorganisms (Fu et al., 2016). Similarly, the concentrations of the yellow particles (organic matter) and the white particles (mineral particles) increased with the concentrations of DAPI-stained bacteria (Fig. 9a), whereas the concentrations of the black particles showed no obvious pattern (Fig. 9a and b). These observations indicate that a close relationship ~~exists~~ existed among DAPI-stained bacteria, organic matter and mineral particles. It is speculated that the yellow particles (organic matter) and the white particles (mineral particles) serve as nutrient ~~sources~~ and shelters for microbes, respectively, and favor their survival and long-distance transport. Some dead cells and debris of microbes are thought to also emit yellow fluorescence (Liu et al., 2014). Furthermore, the concentrations of the black particles decreased in some of the dust events (Fig. 8a), and the concentrations of the DAPI-stained bacteria and the yellow particles showed no obvious relationship with those ~~the concentrations~~ of the black particles, whereas the concentrations of the white particles showed a declining trend with the increasing black-particle concentrations (Fig. 9b). Thus, fewer black particles existed in the dust samples, and the black particles have little connection with the DAPI-stained bacteria and the yellow particles. These results are supported by other field observations in Tsogt-Ovoo of the Gobi Desert of Asia (Maki et al., 2016).

~~The ratio of the concentrations of the DAPI-stained bacteria, the black particles and the white particles to those of the yellow particles were considered together with the charge capacity of the yellow particles. The charge capacity of the yellow particles for the DAPI-stained bacteria increased slightly~~

~~with the concentrations of the yellow particles (Fig. 10a). This result indicates that the yellow particles (organic matter) in the dust may serve as nutrient sources and favor microbial survival, which is also partly confirmed by the micrographs (Fig. 6a, b, c and d). The ratios of the concentrations of the DAPI-stained bacteria, the black particles and the white particles to those of the yellow particles ranged from 5.1% ± 6.3% (non-dust samples) to 9.8% ± 6.3% (dust samples), from 73.6% ± 100.4% (non-dust samples) to 9.0% ± 8.2% (dust samples), and from 2.7% ± 3.3% (non-dust samples) to 3.8% ± 4.1% (dust samples), respectively (Fig. 10b). It is quite clear that the charge capacity of the yellow particles associated with the DAPI-stained bacteria was higher in the dust samples compared with that in the non-dust samples. On the other hand, the charge capacity of the yellow particles associated with the black particles was much lower in the dust samples; thus, greater numbers of bacteria can be contained in a unit of yellow particles during dust events, whereas the black particles displayed the opposite behavior.~~

The concentration ratios of the DAPI-stained bacteria, the black particles and the white particles to the yellow particles were calculated (Fig. 10). The concentration ratios of the DAPI-stained bacteria, the black particles and the white particles to the yellow particles ranged from 5.1% ± 6.3% (non-dust samples) to 9.8% ± 6.3% (dust samples), from 73.6% ± 100.4% (non-dust samples) to 9.0% ± 8.2% (dust samples), and from 2.7% ± 3.3% (non-dust samples) to 3.8% ± 4.1% (dust samples), respectively (Fig. 10b). The concentration ratios of the DAPI-stained bacteria to the yellow particles were much higher in the dust samples than in the non-dust samples, while the concentration ratios of the black particles to the yellow particles significantly decreased in the dust samples in comparison to the non-dust samples. Thus, greater numbers of bacteria can be contained in a unit of yellow particles during

dust events, whereas the black particles displayed the opposite behavior. The results indicate that the yellow particles (organic matter) in the dust may serve as nutrient and favor microbial survival and long-distance transport, which was also partly confirmed by the micrographs (Fig. 6a, b, c and d). In contrast, anthropogenic black carbon load in the dust samples decreased significantly comparing to non-dust samples.

3.4 Alpha and beta diversity analysis of the samples

The 16S rDNA sequences from 22 samples were divided into 28,949 OTUs (sequences with > 97% similarity), and the number of OTUs contained in these samples ranged from 150 to 3147 (Fig. 11a). On the other hand, the ITS rDNA sequences from 18 of the samples were divided into 223 OTUs, and the number of OTUs contained in these samples ranged from 5 to 74 (Fig. 11b). Phylogenetic assignment of the 16S rDNA sequences resulted in an overall diversity profile that included bacteria and archaea, 34 phyla and candidate divisions, 94 classes (and class-level candidate taxa), 166 orders (and ~~class~~order-level candidate taxa), and 243 families (and family-level candidate taxa). Phylogenetic assignment of the ITS rDNA sequences resulted in an overall diversity profile that included 3 phyla (*Ascomycota*, *Basidiomycota*, and *Chytridiomycota*), 19 classes (and class-level candidate taxa), 62 orders (and ~~class~~order-level candidate taxa), and 149 families (and family-level candidate taxa). Overall, the alpha diversity of the bacteria in the dust samples was higher than that of non-dust samples collected in Erenhot (Fig. 12a), whereas the alpha diversity of the fungi was much lower and showed no obvious pattern between the dust and non-dust samples (Fig. 12b). The results from another study in South Korea also suggest that airborne bacterial diversity (at least the richness index) ~~is~~ increased during

Asian dust events (Cha et al., 2016). It illustrates that the dust events can carry not only a huge number of bacteria, but also a great variety of that.

To analyze similarities in the bacterial community contained in each sample, principal coordinates analysis (PCoA) with weighted UniFrac distances was carried out. The sample "Dz5_5R100" was discarded before PCoA analysis, due to the small number of OTUs it contained (Fig. 11a). The results indicate that the dust and non-dust samples from Erenhot displayed a distinct separation (Fig. 13), which indicates that the bacterial community compositions differed significantly between the dust and non-dust samples. Similarly, the distinct clustering of prokaryotic communities separating dust and non-dust samples of Tsogt-Ovoo was found in another study (Maki et al., 2016). Furthermore, the dust samples collected in Erenhot showed a high degree of similarity with the samples of R-DzToUb, which suggests that some types of bacteria were transported from the Gobi Desert of Mongolia to Erenhot.

3.5 Analysis of the microbial community composition in the dust events and non-dust events

Comparative analysis of the bacterial community composition revealed that the ubiquitous bacterial phyla in the samples ~~air~~ were *Acidobacteria*, *Actinobacteria*, *Bacteroidetes*, *Chloroflexi*, *Firmicutes*, *Gemmatimonadetes*, and *Proteobacteria* (Fig. ~~S4~~S5), which are typically the most abundant phyla in the atmospheric environment of the Gobi Desert of Asia (Maki et al., 2016). Of these phyla, *Actinobacteria*, *Bacteroidetes*, *Proteobacteria* remained the dominant phyla in all the samples (Fig. 14).

At the phylum level, as for Erenhot, the relative abundances ~~amounts~~ of *Acidobacteria* and *Chloroflexi* in the dust samples ~~have~~ had a remarkable rise compared with the non-dust samples, ~~and the next were~~ followed by *Crenarchaeota*, *Firmicutes* and *Proteobacteria* (Fig. 14a, ~~and~~ b and Fig. S5a). By contrast, opposite phenomenon appeared in R-DzToUb, and the relative abundances ~~amounts~~ of

Acidobacteria, *Chloroflexi* in the non-dust samples were greater than ~~that~~ those in the dust samples (Fig. 14c and d). ~~The class *Chloroflexi* was dominating among the members of this phylum (Fig. 14 and 15).~~ It is~~'s~~ worth noting that all samples (dust and non-dust samples) of R-DzToUb were collected on the road from Dalanzadgad to Ulaanbaatar, small dust events continuously occurred there and some residues of dust particles would be remained in the air for a longer period. The class *Chloroflexi* was the dominating among the members of this phylum (Fig. 14 and 15). Notably, the phylum *Chloroflexi* includes six classes, of which only the class *Chloroflexi* consists of phototrophic bacteria. This phototrophic group, called filamentous anoxygenic phototrophic bacteria, shares the following features in common: multicellular filamentous morphology, gliding motility, and anoxygenic photosynthetic activity (Hanada, 2014). This phototrophic group could obtain light energy and keep their survival in the air, using the light for photosynthesis. Long-distance transmission of such group is possible.

The relative abundance ~~amounts~~ of *Proteobacteria* in all dust samples increased slightly compared with non-dust samples, and ~~among this group~~ *Alphaproteobacteria* made the major contribution among this group, by contrast, *Gammaproteobacteria* was just the reverse (Fig. 14 and 15). It suggests that the relative abundance ~~amounts~~ of *Alphaproteobacteria* in the dust ~~are~~ was higher than that in the air. These bacteria could help to identify the mixture levels of air masses transported for long distances, even the relative contributions of local sources and remote sources (particularly deserts) to the concentration of airborne biological particles in different regions (Maki et al., 2017).

The relative abundance of *Firmicutes* increased slightly in the dust samples compared with the non-dust samples (Fig. 14). *Firmicutes* was the predominant phylum of surface sand samples in the Gobi Desert of Asia, but not in the Taklamaken Desert (An et al., 2013). The relative abundance of

Firmicutes could reach as high as 82% in the surface sand samples from the Gobi Desert of Asia (44.3°N, 110.1°E) (An et al., 2013), but it was found in relatively small proportions that did not exceed 5% in all the air samples (Fig. 14). Maki et al. (2016) found that the relative abundance of *Firmicutes* in air samples from the Gobi Desert of Asia (44.2304°N, 105.1700°E) varied greatly, from 15.7 to 40.5% in non-dust samples, and no more than 12% in dust samples. The sequences of *Firmicutes* mainly belonged to the classes *Bacilli* and *Clostridia* in air samples from Tsogt-Ovoo, Mongolia (Maki et al., 2016). While *Bacilli*, *Clostridia* and *Erysipelotrichi* in the phylum *Firmicutes* were found in the air samples from Erenhot (Fig. S5). The averaged relative abundance of *Bacilli* in dust samples from Erenhot was 3.2%, while it is much lower in non-dust samples (Fig. 15). It is worth mentioning that Zhu et al. (2018) found that the averaged relative abundance of *Firmicutes* in cloud samples at Mt. Tai of China was 80.5%. As for the Taklimakan Desert, Puspitasari et al. (2015) analyzed the bacterial diversity in sand dunes and dust aerosol, and the relative abundance of *Firmicutes* in dust aerosol samples was higher than that in surface sand samples, which shows a different pattern comparing to the Gobi Desert of Asia. In conclusion, the bacterial community compositions in the air are different from that in the surface sand or soil, and differ by the location and transmitting vector.

~~At the class level, *Chloracidobacteria* and *Gemmatimonadetes* in dust samples of Erenhot and non-dust samples of R-DzToUb have higher relative amounts compared with non-dust samples of Erenhot and dust samples of R-DzToUb (Fig. 15). *Cytophagia* in the phylum *Bacteroidetes* shows similar phenomenon. Further, *Bacilli* in non-dust samples of Erenhot shows very low amounts down to the detection limit, whereas its relative amounts in other samples keep stable.~~

In addition, two phyla in the archaea kingdom, *Crenarchaeota* (which contains *Thaumarchaeota* at the class level) and *Euryarchaeota* (which contains *Methanobacteria*, *Thermoplasmata*, *Methanomicrobia* and *Halobacteria*), were detected, but their relative abundances were ~~relatively~~ much lower ~~compared~~ comparing to the dominant bacterial phyla. Particularly, *Thaumarchaeota* was found only in the samples "ER3_31N" (heavy dust event) and "Dz5_5R600" (the dust source region) in proportions exceeding 2% (Fig. ~~S4~~S5)~~, which implies that it may be used as an air mass tracer of dust events~~. These bacteria ~~may~~ could be used as tracers of air masses during dust events, even used to distinguish the dust that has been transported over a long distance from local dust.

~~Furthermore, *Firmicutes* was the predominant phylum in the Gobi Desert. The proportions of this phylum reach as high as 82% in surface sand samples, but it was found in relatively small proportions that did not exceed 5% in the air samples (Fig. 14). It's clear that the bacterial community composition in the air is very different from that in the surface sand or soil.~~

The predominant fungal phyla were *Ascomycota* (mainly *Dothideomycetes* and *Sordariomycetes*) and *Basidiomycota* (mainly *Agaricomycetes*), and there was also much lower relative abundance ~~amount~~ of *Chytridiomycota* (Fig. ~~S5~~S6). There is no obvious pattern of the predominant fungal phyla in the dust and non-dust samples. At the class level, *Agaricomycetes*, *Dothideomycetes* and *Sordariomycetes* were the predominant, and the dust samples contained more diverse fungal classes than the non-dust samples (Fig. 16). As for Erenhot, the relative abundances ~~amounts~~ of *Microbotryomycetes*, *Pucciniomycetes* and *Tremellomycetes* in the dust samples increased significantly compared with ~~that~~ those ~~of~~ in the non-dust samples. While the relative abundance ~~amounts~~ of *Eurotiomycetes* in the dust samples of R-DzToUb had a remarkable boom, in the meantime, that of

带格式的: 字体: 倾斜

带格式的: 字体: 非倾斜

Agaricomycetes almost halved in the dust samples, comparing to~~with that of~~ the non-dust samples there. In conclusion, there ~~are~~ were obvious differences of the fungal community compositions between the dust and non-dust samples, and the changing pattern may be diversiform within different locations.

4 Conclusion

During the DuBi-2016 campaign, bioaerosol samples were continuously collected along the transport path of Asian dust, and the effects of dust events originating in the Gobi Desert of Asia on the amount~~s~~ and diversity of bioaerosols were investigated. The concentrations of DAPI-stained bacteria in the dust samples can reach two orders of magnitude greater than those observed in the non-dust samples and three orders of magnitude greater for the yellow particles (organic matter). In addition, the alpha diversity of the bacteria in the dust samples was also greater than that noted in the non-dust samples. In conclusion, both the number of bacteria and the diversity of the bacterial communities increased significantly during the dust events, as determined by means of microscopic observations made with DAPI staining and MiSeq sequencing analysis. The results indicate ~~It indicates~~ that dust events can carry a surprising number of highly diverse microbes to downwind regions, and this transport may have potentially important impacts on local ecological environments ~~conditions~~ and climate change.

Although deserts likely play a less important role as a source of biological matter to the atmosphere than do biologically active regions, the atmospheric residence time of particles emitted from deserts is much longer than that of ~~for~~ most other source regions as a result of the combination of strong dry convection and a lack of removal by precipitation in desert regions (Burrows et al., 2009; Schulz et al., 1998). So bioaerosols in the desert dust particles ~~emitted there~~ are more likely to participate in long-

distance transport and be observed in other regions. During the long-distance transport period, airborne microbes employ diverse strategies to adapt to the harsh atmospheric environment and maintain their viability. Microbial activities, including reproductive activity, may take place in the air, as were partly established by microscopic and SEM observations. Reproductive activity increases the number of microbes in the air, which may lead to underestimation of the concentrations of microbes. Some activities may change the physicochemical properties of other atmospheric components, such as secondary organic aerosols, thereby changing their capacity to serve as ice nuclei (INs) or cloud condensation nuclei (CCNs), their radiative properties and their other characteristics.

The predominant bacterial phyla found in the air samples were *Actinobacteria*, *Bacteroidetes*, *Proteobacteria*. Many bacterial members can enter the atmosphere with the aid of wind. Some bacterial members display no resistance to the harsh environmental stressors in the atmosphere and are eliminated mostly; on the other hand, the remainder can be transported over long distances on the wind and have long-term impacts on ecological environments and climate change. *Firmicutes* provides a good example; it was found in large proportions that may even reach 82% at the surface of the Gobi Desert of Asia. However, most of them were eliminated by environmental stressors, and only a small fraction remained and the relative abundance ~~amounts~~ in the air was ~~were~~ less than 5%. Moreover, the relative abundances ~~amounts~~ of some bacterial members and fungal members increased markedly, together with the higher alpha diversity in dust samples than that in non-dust samples, which contributed to a high diversity of the bacterial community in the downwind atmosphere, potentially representing a threat to local ecological environments.

Naturally, the dust and non-dust samples could be clearly separated from each other, due to the different ~~differing~~ compositions of the bacterial communities they contained. In addition, some bacteria and fungi were only found in the dust samples. These taxa may originate in the dust source regions and can be used for provenance tracking, particularly to distinguish dust transported over long distances from local dust.

Bioaerosols originating from Asian desert areas have high possibility to disperse to downwind regions, such as Korea and Japan, by the prevailing westerly winds in the middle latitudes (Iwasaka et al., 2009) and are sometimes carried to the Pacific Ocean (Smith et al., 2013). Huge dust events create an atmospheric bridge over land and sea, which may contribute to the biodiversity on the earth, but the impact of bioaerosols transported over long distance should be checked carefully.

Although the amount and diversity of bioaerosols in the air have been investigated, the viability and activity of airborne microbes, the interactions between bioaerosols and other gaseous and solid components in the air, and the effects of bioaerosols on animals and plants, the ecological environment and the climate system require in-depth study to permit a detailed understanding of bioaerosols in the air.

Acknowledgments

This research was supported by the National Natural Science Foundation of China (41575017, 41375031, 41521004, 41405113 and 41505011), a China 111 project (B 13045), ~~and~~ the Fundamental Research Funds for the Central Universities (lzujbky-2017-k03 and lzujbky-2017-it21) and the Foundation of Key Laboratory for Semi-Arid Climate Change of the Ministry of Education in Lanzhou University. This study was also supported by Grants-in-Aid for Scientific Research (A) (No. 17H01616) and (B) (No. 26304003) from the Japan Society for the Promotion of Science (JSPS). The employees of

Fasmac Co., Ltd. assisted in the MiSeq sequencing analyses. Air mass trajectories were reconstructed using the NOAA ARL website (http://ready.arl.noaa.gov). We wish to thank the Electron Microscopy Centre of Lanzhou University for the microscopy and microanalysis of our specimens.

带格式的: 英语(英国)

References

Amato, P., Joly, M., Schaupp, C., Attard, E., Möhler, O., Morris, C. E., Brunet, Y. and Delort, A. M.: Survival and ice nucleation activity of bacteria as aerosols in a cloud simulation chamber, Atmos. Chem. Phys., 15(11), 6455–6465, doi:10.5194/acp-15-6455-2015, 2015.

An, S., Couteau, C., Luo, F., Neveu, J. and DuBow, M. S.: Bacterial diversity of surface sand samples from the Gobi and Taklamaken deserts, Microb Ecol, 66(4), 850–860, doi:10.1007/s00248-013-0276-2, 2013.

Bi, J., Huang, J., Holben, B. and Zhang, G.: Comparison of key absorption and optical properties between pure and transported anthropogenic dust over East and Central Asia, Atmos. Chem. Phys., 16(24), 15501–15516, doi:10.5194/acp-16-15501-2016, 2016.

Bi, J., Huang, J., Shi, J., Hu, Z., Zhou, T., Zhang, G., Huang, Z., Wang, X. and Jin, H.: Measurement of scattering and absorption properties of dust aerosol in a Gobi farmland region of northwestern China - A potential anthropogenic influence, Atmos. Chem. Phys., 17(12), 7775–7792, doi:10.5194/acp-17-7775-2017, 2017.

Bory, A. J.-M., Biscaye, P. E. and Grousset, F. E.: Two distinct seasonal Asian source regions for mineral dust deposited in Greenland (NorthGRIP), Geophys. Res. Lett., 30(4), 1167, doi:10.1029/2002GL016446, 2003.

Brown, J. K. M. and Hovmøller, M. S.: Aerial Dispersal of Pathogens on the Global and Continental Scales and Its Impact on Plant Disease, Science., 297(5581), 537–541, doi:10.1126/science.1072678, 2002.

Burrows, S. M., Elbert, W., Lawrence, M. G. and Pöschl, U.: Bacteria in the global atmosphere – Part 2: Modeling of emissions and transport between different ecosystems, Atmos. Chem. Phys., 9(1987), 9263–9280, doi:10.5194/acp-9-9263-2009, 2009.

Caporaso, J. G., Lauber, C. L., Walters, W. A., Berg-Lyons, D., Lozupone, C. A., Turnbaugh, P. J., Fierer, N. and Knight, R.: Global patterns of 16S rRNA diversity at a depth of millions of sequences per sample, Proc Natl Acad Sci U S A, 108 Suppl, 4516–4522, doi:10.1073/pnas.1000080107, 2011.

Cha, S., Lee, D., Jang, J. H., Lim, S., Yang, D. and Seo, T.: Alterations in the airborne bacterial community during Asian dust events occurring between February and March 2015 in South Korea, Sci. Rep., 6(April), 1–9, doi:10.1038/srep37271, 2016.

Cha, S., Srinivasan, S., Jang, J. H., Lee, D., Lim, S., Kim, K. S., Jheong, W., Lee, D. W., Park, E. R., Chung, H. M., Choe, J., Kim, M. K. and Seo, T.: Metagenomic analysis of airborne bacterial community and diversity in seoul, korea, during December 2014, asian dust event, PLoS One, 12(1), 1–12, doi:10.1371/journal.pone.0170693, 2017.

Chen, S., Huang, J., Li, J., Jia, R., Jiang, N., Kang, L., Ma, X. and Xie, T.: Comparison of dust emissions, transport, and deposition between the Taklimakan Desert and Gobi Desert from 2007 to 2011, Sci. China Earth Sci., 60(7), 1338–1355, doi:10.1007/s11430-016-9051-0, 2017.

Creamean, J. M., Suski, K. J., Rosenfeld, D., Cazorla, A., Demott, P. J., Sullivan, R. C., White, A. B., Ralph, F., Minnis, P., Comstock, J. M., Tomlinson, J. M. and Prather, K. A.: Dust and Biological Aerosols from the Sahara and Asia Influence Precipitation in the Western U.S., Science, 339(6127), 1572–1578, doi:10.1126/science.1227279, 2013.

DeLeon-Rodriguez, N., Lathem, T. L., Rodriguez, R. L., Barazesh, J. M., Anderson, B. E., Beyersdorf, A. J., Ziemba, L. D., Bergin, M., Nenes, A. and Konstantinidis, K. T.: Microbiome of the upper troposphere: species composition and prevalence, effects of tropical storms, and atmospheric implications, Proc Natl Acad Sci U S A, 110(7), 2575–2580, doi:10.1073/pnas.1212089110, 2013.

Dong, L., Qi, J., Shao, C., Zhong, X., Gao, D., Cao, W., Gao, J., Bai, R., Long, G. and Chu, C.: Concentration and size distribution of total airborne microbes in hazy and foggy weather, Sci. Total Environ., 541, 1011–1018, doi:10.1016/j.scitotenv.2015.10.001, 2016.

Fröhlich-Nowoisky, J., Kampf, C. J., Weber, B., Huffman, J. A., Pöhlker, C., Andreae, M. O., Lang-Yona, N., Burrows, S. M., Gunthe, S. S., Elbert, W., Su, H., Hoor, P., Thines, E., Hoffmann, T., Després, V. R. and Pöschl, U.: Bioaerosols in the Earth System: Climate, Health, and Ecosystem Interactions, Atmos. Res., 182, 346-376, doi:10.1016/j.atmosres.2016.07.018, 2016.

Fu, P. Q., Zhuang, G. S., Sun, Y. L., Wang, Q. Z., Chen, J., Ren, L. J., Yang, F., Wang, Z. F., Pan, X. L., Li, X. D. and Kawamura, K.: Molecular markers of biomass burning, fungal spores and biogenic SOA in the Taklimakan desert aerosols, Atmos. Environ., 130, 64–73, doi:10.1016/j.atmosenv.2015.10.087, 2016.

Griffin, D. W.: Atmospheric movement of microorganisms in clouds of desert dust and implications for human health, Clin. Microbiol. Rev., 20(3), 459–477, doi:10.1128/CMR.00039-06, 2007.

Grousset, F. E., Ginoux, P., Bory, A. and Biscaye, P. E.: Case study of a Chinese dust plume reaching the French Alps, Geophys. Res. Lett., 30(6), 1277, doi:10.1029/2002GL016833, 2003.

Hanada S.: The phylum Chloroflexi, the family Chloroflexaceae, and the related phototrophic families Oscillochloridaceae and Roseiflexaceae: The Prokaryotes, Springer, Berlin Heidelberg, Germany, 515-532, 2014.

Hara, K. and Zhang, D.: Bacterial abundance and viability in long-range transported dust, Atmos. Environ., 47, 20–25, doi:10.1016/j.atmosenv.2011.11.050, 2012.

Hervàs, A., Camarero, L., Reche, I. and Casamayor, E. O.: Viability and potential for immigration of airborne bacteria from Africa that reach high mountain lakes in Europe, Environ. Microbiol., 11(6), 1612–1623, doi:10.1111/j.1462-2920.2009.01926.x, 2009.

Ho, H. M., Rao, C. Y., Hsu, H. H., Chiu, Y. H., Liu, C. M. and Chao, H. J.: Characteristics and determinants of ambient fungal spores in Hualien, Taiwan, Atmos. Environ., 39(32), 5839–5850, doi:10.1016/j.atmosenv.2005.06.034, 2005.

Hua, N. P., Kobayashi, F., Iwasaka, Y., Shi, G. Y. and Naganuma, T.: Detailed identification of desert-originated bacteria carried by Asian dust storms to Japan, Aerobiologia (Bologna)., 23(4), 291–298, doi:10.1007/s10453-007-9076-9, 2007.

Huang, J., Minnis, P., Chen, B., Huang, Z., Liu, Z., Zhao, Q., Yi, Y. and Ayers, J. K.: Long-range transport and vertical structure of Asian dust from CALIPSO and surface measurements during PACDEX, J. Geophys. Res. Atmos., 113(23), 1–13, doi:10.1029/2008JD010620, 2008a.

Huang, J., Zhang, W., Zuo, J., Bi, J., Shi, J., Wang, X., Chang, Z., Huang, Z., Yang, S., Zhang, B., Wang, G., Feng, G., Yuan, J., Zhang, L., Zuo, H., Wang, S., Fu, C., and Chou, J.: An overview of the semi-arid climate and environment research observatory over the Loess Plateau, Adv. Atmos. Sci., 25(6), 906–921, doi: 10.1007/s00376-008-0906-7, 2008b.

Huang, J., Fu, Q., Zhang, W., Wang, X., Zhang, R., Ye, H. and Warren, S. G.: Dust and black carbon in seasonal snow across Northern China, Bull. Am. Meteorol. Soc., 92(2), 175–181, doi:10.1175/2010BAMS3064.1, 2011.

Huang, J., Yu, H., Guan, X., Wang, G. and Guo, R.: Accelerated dryland expansion under climate change, Nat. Clim. Chang., doi:10.1038/nclimate2837, 2015.

Huang, J., Li, Y., Fu, C., Chen, F., Fu, Q., Dai, A., Shinoda, M., Ma, Z., Guo, W., Li, Z., Zhang, L., Liu, Y., Yu, H., He, Y., Xie, Y., Guan, X., Ji, M., Lin, L., Wang, S., Yan, H. and Wang, G.: Dryland Climate Change: Recent Progress and Challenges, Rev. Geophys., 1–60, doi:10.1002/2016RG000550, 2017a.

Huang, J., Yu, H., Dai, A., Wei, Y. and Kang, L.: Drylands face potential threat under 2 °C global warming target, Nat. Clim. Chang., (April), doi:10.1038/nclimate3275, 2017b.

Huang, Z., Huang, J., Bi, J., Wang, G., Wang, W., Fu, Q., Li, Z., Tsay, S.-C. and Shi, J.: Dust aerosol vertical structure measurements using three MPL lidars during 2008 China-U.S. joint dust field experiment, J. Geophys. Res., 115, D00K15, doi:10.1029/2009JD013273, 2010.

Huang Z, Huang J, Hayasaka T, Wang S, Zhou T, Jin H.: Short-cut transport path for Asian dust directly to the Arctic: a case study, Environmental Research Letters., 10(11):114018, doi:10.1088/1748-9326/10/11/114018, 2015.

Husar, R. B., Tratt, D. M., Schichtel, B. A., Falke, S. R., Li, F., Jaffe, D., Gill, T., Laulainen, N. S., Lu, F., Reheis, M. C., Chun, Y., Westphal, D., Mckendry, I., Kuring, N., Feldman, G. C., Frouin, R. J., Merrill, J., Dubois, D., Vignola, F., Murayama, T., Nickovic, S., Wilson, W. E., Sassen, K., Sugimoto, N. and Malm, W. C.: Asian dust events of April 1998, J. Geophys. Res. Atmos., 106(D16), 18317–18330, doi:10.1029/2000JD900788, 2001.

Ichinose, T., Nishikawa, M., Takano, H., Sera, N., Sadakane, K., Mori, I., Yanagisawa, R., Oda, T., Tamura, H., Hiyoshi, K., Quan, H., Tomura, S. and Shibamoto, T.: Pulmonary toxicity induced by intratracheal instillation of Asian yellow dust (Kosa) in mice, Env. Toxicol Pharmacol, 20(1), 48–56, doi:10.1016/j.etap.2004.10.009, 2005.

Iwasaka, Y., Hiroaki, M. and Nagaya, K.: The transport and spatial scale of Asian dust storm clouds: a case study of the dust storm event of April 1979, Tellus, 35B, 189–196, doi:10.3402/tellusb.v35i3.14594, 1983.

Iwasaka, Y., Shi, G. Y., Yamada, M., Kobayashi, F., Kakikawa, M., Maki, T., Naganuma, T., Chen, B., Tobo, Y. and Hong, C. S.: Mixture of Kosa (Asian dust) and bioaerosols detected in the atmosphere over the Kosa particles source regions with balloon-borne measurements: possibility of long-range transport, Air Qual. Atmos. Heal., 2(1), 29–38, doi:10.1007/s11869-009-0031-5, 2009.

Jeon, E. M., Kim, H. J., Jung, K., Kim, J. H., Kim, M. Y., Kim, Y. P. and Ka, J.-O.: Impact of Asian dust events on airborne bacterial community assessed by molecular analyses, Atmos. Environ., 45(25), 4313–4321, doi:10.1016/j.atmosenv.2010.11.054, 2011.

Jeon, E. M., Kim, Y. P., Jeong, K., Kim, I. S., Eom, S. W., Choi, Y. Z. and Ka, J. O.: Impacts of Asian dust events on atmospheric fungal communities, Atmos. Environ., 81, 39–50, doi:10.1016/j.atmosenv.2013.08.039, 2013.

~~Jianping, H. and Xin, W.: An Overview of the Semi-arid Climate and Environment Research Observatory over the Loess Plateau á è, Adv. Atmos. Sci., 25(6), 906–921, doi:10.1007/s00376-008-0906-7.1.Introduction, 2008.~~

Jorquera, H., Borzutzky, A., Hoyos-Bachiloglu, R. and García, A.: Association of Kawasaki disease with tropospheric winds in Central Chile: Is wind-borne desert dust a risk factor ?, Environ. Int., 78, 32–38, doi:10.1016/j.envint.2015.02.007, 2015.

Liu, B., Ichinose, T., He, M., Kobayashi, F., Maki, T., Yoshida, S., Yoshida, Y., Arashidani, K., Takano, H., Nishikawa, M., Sun, G. and Shibamoto, T.: Lung inflammation by fungus, Bjerkandera adusta isolated from Asian sand dust (ASD) aerosol and enhancement of ovalbumin-induced lung eosinophilia by ASD and the fungus in mice., Allergy Asthma. Clin. Immunol., 10(1), 10, doi:10.1186/1710-1492-10-10, 2014.

Lozupone, C., Lladser, M. E., Knights, D., Stombaugh, J. and Knight, R.: UniFrac: An effective distance metric for microbial community comparison, ISME J., 5(2), 169–172, doi:10.1038/ismej.2010.133, 2011.

Lozupone, C. A., Hamady, M., Kelley, S. T. and Knight, R.: Quantitative and qualitative ?? diversity measures lead to different insights into factors that structure microbial communities, Appl. Environ. Microbiol., 73(5), 1576–1585, doi:10.1128/AEM.01996-06, 2007.

Maki, L. R. and Willoughby, K. J.: Bacteria as Biogenic Sources of Freezing Nuclei, J. Appl. Meteorol., 17(7), 1049–1053, doi:10.1175/1520-0450(1978)017<1049:BABSOF>2.0.CO;2, 1978.

Maki, T., Susuki, S., Kobayashi, F., Kakikawa, M., Yamada, M., Higashi, T., Chen, B., Shi, G., Hong, C., Tobo, Y., Hasegawa, H., Ueda, K. and Iwasaka, Y.: Phylogenetic diversity and vertical distribution of a halobacterial community in the atmosphere of an Asian dust (KOSA) source region, Dunhuang City, Air Qual. Atmos. Heal., 1(2), 81–89, doi:10.1007/s11869-008-0016-9, 2008.

Maki, T., Puspitasari, F., Hara, K., Yamada, M., Kobayashi, F., Hasegawa, H. and Iwasaka, Y.: Variations in the structure of airborne bacterial communities in a downwind area during an Asian dust (Kosa) event, Sci Total Env., 488–489, 75–84, doi:10.1016/j.scitotenv.2014.04.044, 2014.

Maki, T., Hara, K., Kobayashi, F., Kurosaki, Y., Kakikawa, M., Matsuki, A., Chen, B., Shi, G., Hasegawa, H. and Iwasaka, Y.: Vertical distribution of airborne bacterial communities in an Asian-dust downwind area, Noto Peninsula, Atmos. Environ., 119, 282–293, doi:10.1016/j.atmosenv.2015.08.052, 2015.

Maki, T., Kurosaki, Y., Onishi, K., Lee, K. C., Pointing, S. B., Jugder, D., Yamanaka, N., Hasegawa, H. and Shinoda, M.: Variations in the structure of airborne bacterial communities in Tsogt-Ovoo of Gobi desert area during dust events, Air Qual. Atmos. Heal., 10(3), 249-260, doi:10.1007/s11869-016-0430-3, 2016.

Maki, T., Hara, K., Iwata, A., Lee, K. C., Kawai, K., Kai, K., Kobayashi, F., Pointing, S. B., Archer, S., Hasegawa, H. and Iwasaka, Y.: Variations in airborne bacterial communities at high altitudes over the Noto Peninsula (Japan) in response to Asian dust events, Atmos. Chem. Phys. ~~Discuss., (January)~~, 17, 11877–11897~~1–32~~, doi:10.5194/acp-17-11877-2017~~/acp-2016-1095~~, 2017.

Nishizawa, T., Sugimoto, N., Matsui, I., Shimizu, A., Hara, Y., Itsushi, U., Yasunaga, K., Kudo, R. and Kim, S. W.: Ground-based network observation using Mie-Raman lidars and multi-wavelength Raman lidars and algorithm to retrieve distributions of aerosol components, J. Quant. Spectrosc. Radiat. Transf., 188, 79–93, doi:10.1016/j.jqsrt.2016.06.031, 2016.

Park, J., Ichijo, T., Nasu, M. and Yamaguchi, N.: Investigation of bacterial effects of Asian dust events through comparison with seasonal variability in outdoor airborne bacterial community, Sci. Rep., 6(May), 35706, doi:10.1038/srep35706, 2016.

Prospero, J. M., Blades, E., Mathison, G. and Naidu, R.: Interhemispheric transport of viable fungi and bacteria from Africa to the Caribbean with soil dust, Aerobiologia (Bologna)., 21(1), 1–19, doi:10.1007/s10453-004-5872-7, 2005.

Pu, W., Wang, X., Zhang, X., Ren, Y., Shi, J. Sen, Bi, J. R. and Zhang, B. D.: Size distribution and optical properties of particulate matter (PM_{10}) and black carbon (BC) during dust storms and local air pollution events across a loess plateau site, Aerosol Air Qual. Res., 15(6), 2212–2224, doi:10.4209/aaqr.2015.02.0109, 2015.

带格式的: 下标

Rodo, X., Ballester, J., Cayan, D., Melish, M. E., Nakamura, Y., Uehara, R. and Burns, J. C.: Association of Kawasaki disease with tropospheric wind patterns, Sci Rep, 1, 152, doi:10.1038/srep00152, 2011.

Schulz, M., Balkanski, Y. J., Guelle, W. and Dulac, F.: Role of aerosol size distribution and source location in a three-dimensional simulation of a Saharan dust episode tested against satellite-derived optical thickness, J. Geophys. Res. Atmos., 103(D9), 10579–10592, doi:10.1029/97JD02779, 1998.

Shimizu, A., Nishizawa, T., Jin, Y., Kim, S.-W., Wang, Z., Batdorj, D. and Sugimoto, N.: Evolution of a lidar network for tropospheric aerosol detection in East Asia, Opt. Eng., 56(3), 31219, doi:10.1117/1.OE.56.3.031219, 2016.

Smets, W., Moretti, S., Denys, S. and Lebeer, S.: Airborne bacteria in the atmosphere: Presence, purpose, and potential, Atmos. Environ., 139, 214–221, doi:10.1016/j.atmosenv.2016.05.038, 2016.

Smith, D. J., Timonen, H. J., Jaffe, D. A., Griffin, D. W., Birmele, M. N., Perry, K. D., Ward, P. D. and Roberts, M. S.: Intercontinental dispersal of bacteria and archaea by transpacific winds, Appl. Environ. Microbiol., 79(4), 1134–1139, doi:10.1128/AEM.03029-12, 2013.

Sugimoto, N., Huang, Z., Nishizawa, T., Matsui, I., and Tatarov, B.: Fluorescence from atmospheric aerosols observed with a multi-channel lidar spectrometer, Optics Express, 20(19), 20800-20807. 2012

Sugimoto, N., and Huang Z.: Lidar methods for observing mineral dust. J. Meteor. Res., 28(2), 173-184, doi: 10.1007/s13351-014-3068-9, 2014.

Tong, Y. and Lighthart, B.: The annual bacterial particle concentration and size distribution in the ambient atmosphere in a rural area of the Willamette Valley, Oregon, Aerosol Sci. Technol., 32(5), 393–403, doi:10.1080/027868200303533, 2000.

Uno, I., Eguchi, K., Yumimoto, K., Takemura, T., Shimizu, A., Uematsu, M., Liu, Z., Wang, Z., Hara, Y. and Sugimoto, N.: Asian dust transported one full circuit around the globe, Nat. Geosci., 2(8), 557–560, doi:10.1038/ngeo583, 2009.

Wang, G., Huang, J., Guo, W., Zuo, J., Wang, J., Bi, J., Huang, Z. and Shi, J.: Observation analysis of land-atmosphere interactions over the Loess Plateau of northwest China, J. Geophys. Res. Atmos., 115(16), 1–15, doi:10.1029/2009JD013372, 2010.

Wang, X., Xu, B. and Ming J.: An Overview of the Studies on Black Carbon and Mineral Dust Deposition in Snow and Ice Cores in East Asia, J. Meteor. Res., 28(3), 354–370, doi:10.1007/s13351-014-4005-7, 2014.

Wang, X., Pu, W., Shi, J., Bi, J., Zhou, T., Zhang, X. and Ren, Y.: A comparison of the physical and optical properties of anthropogenic air pollutants and mineral dust over Northwest China, J. Meteor. Res., 29(2), 180–200, doi:10.1007/s13351-015-4092-0, 2015.

Wang, X., Wen, H., Shi, J., Bi, J., Huang, Z., Zhang, B., Zhou, T., Fu, K., Chen, Q. and Xin, J.: Optical and microphysical properties of natural mineral dust and anthropogenic soil dust near dust source regions over northwestern China, Atmos. Chem. Phys., 18(3), 2119–2138, doi:10.5194/acp-18-2119-2018, 2018.

Wu, P. C., Tsai, J. C., Li, F. C., Lung, S. C. and Su, H. J.: Increased levels of ambient fungal spores in Taiwan are associated with dust events from China, Atmos. Environ., 38(29), 4879–4886, doi:10.1016/j.atmosenv.2004.05.039, 2004.

Yamaguchi, N., Ichijo, T., Sakotani, A., Baba, T. and Nasu, M.: Global dispersion of bacterial cells on Asian dust, Sci Rep, 2, 525, doi:10.1038/srep00525, 2012.

Yeo, H. G. and Kim, J. H.: SPM and fungal spores in the ambient air of west Korea during the Asian dust (Yellow sand) period, Atmos. Environ., 36(35), 5437–5442, doi:10.1016/S1352-2310(02)00672-6, 2002.

Zhou, T., Huang, J., Huang, Z., Liu, J., Wang, C., Lin, L.: The depolarization-attenuated backscatter relationship for dust plumes, Optics Express, 13(21): 15195-15204, doi: 10.1364/OE.21.015195, 2013.

Zhu, C., Chen, J., Wang, X., Li, J., Wei, M., Xu, C., Xu, X., Ding, A. and Collett, J. L.: Chemical composition and bacterial community in size-resolved cloud water at the summit of Mt. Tai, China, Aerosol Air Qual. Res., 18(1), 1–14, doi:10.4209/aaqr.2016.11.0493, 2018.

Table 1 Information of sampling sites

Location	Latitude (°N) and longitude (°E)	Altitude (ASL*)	Sampling height (AGL*)	Sampling period	Sampling duration
Erenhot	ER: 43.668, 111.953	957 m	20 m (on a building)	2016/3/30 - 2016/5/20	2 h ~24 h
Zhangbei	ZB: 41.156, 114.701	1395 m	4 m (on a container)	2016/3/29 - 2016/5/31	2 h ~16 h
Jinan	JN: 36.673, 117.057	48 m	25 m (on a building)	2016/3/23 - 2016/6/4	10 ~14 h
R-DzToUb	Dz: 43.557, 104.419 Ub: 47.886, 106.906	Dz: 1489 m Ub: 1302 m	2 m (on a car)	2016/5/5	1 h

*ASL: above sea level
*AGL: above ground level

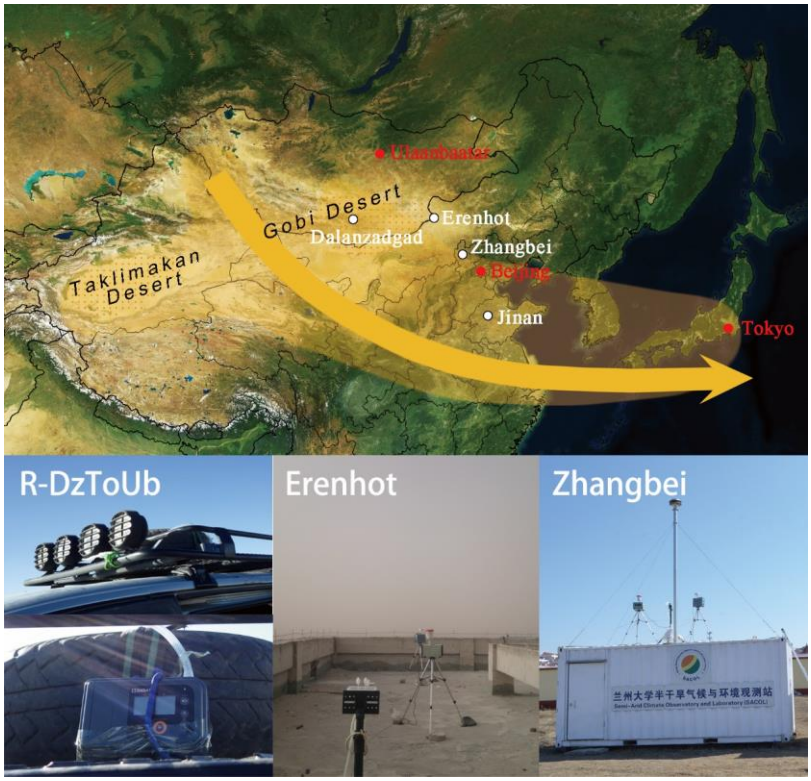

Fig. 1 The design of the Dust-Bioaerosol Campaign in 2016, the locations of the sampling sites and the contexts of the bioaerosol samplers (R-DzToUb is located along the road between Dalanzadgad and Ulaanbaatar).

5

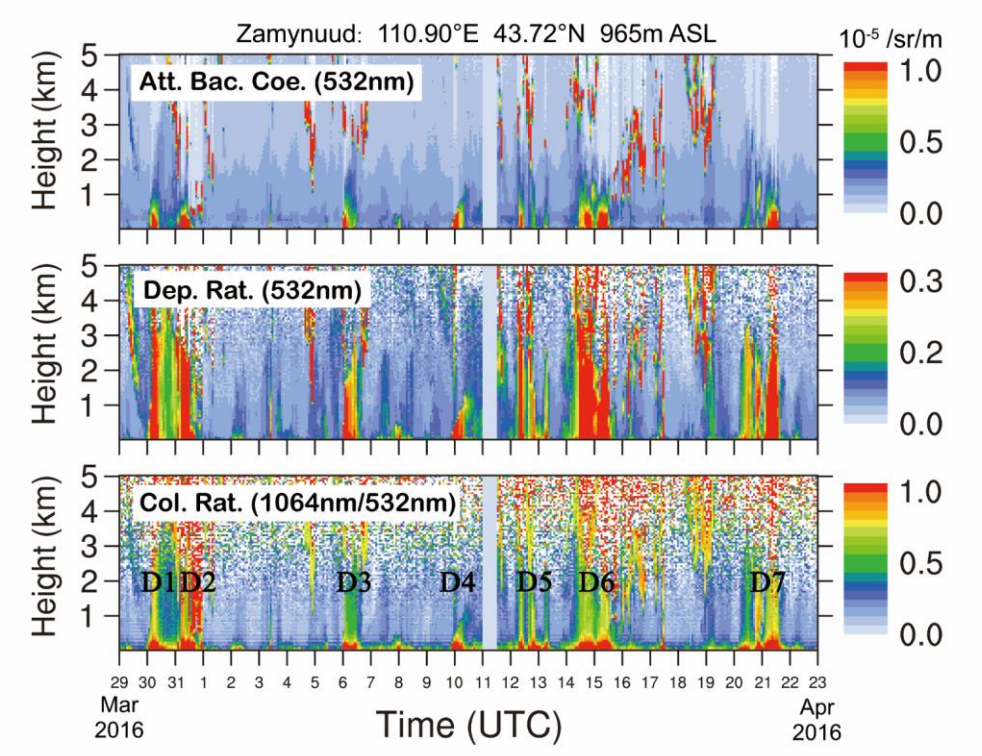

Fig. 2 Li<u>dar</u>~~DAR~~ observations in Zamynuud during the sampling period. D1-D7 represent dust events that occurred in Erenhot.

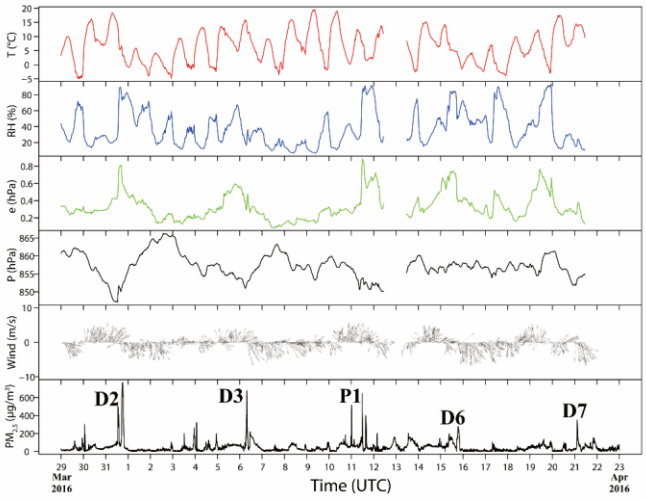

Fig. 3 Meteorological conditions and air quality measurements during the sampling period. T, temperature; RH, relative humidity; e, water vapor pressure; P, atmospheric pressure. D1-D7 correspond to the 7 dust events that occurred in Erenhot.

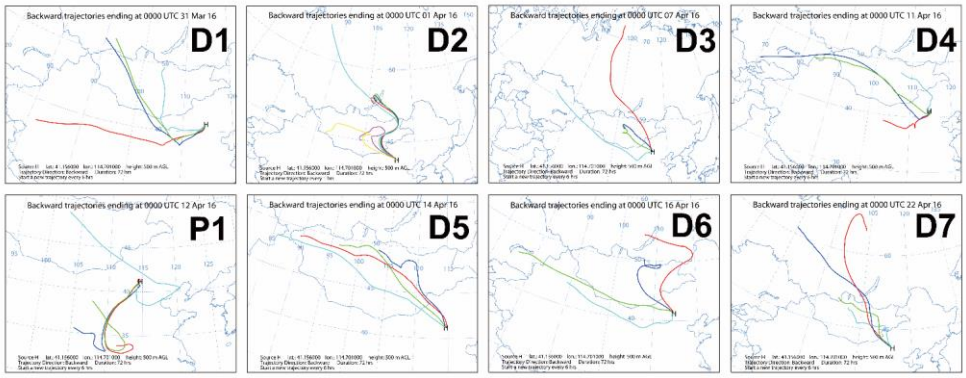

Fig. 4 72-h back trajectories of air masses in Zhangbei calculated using the HYSPLIT model. D1-D7 represent the dust events that occurred in Erenhot.

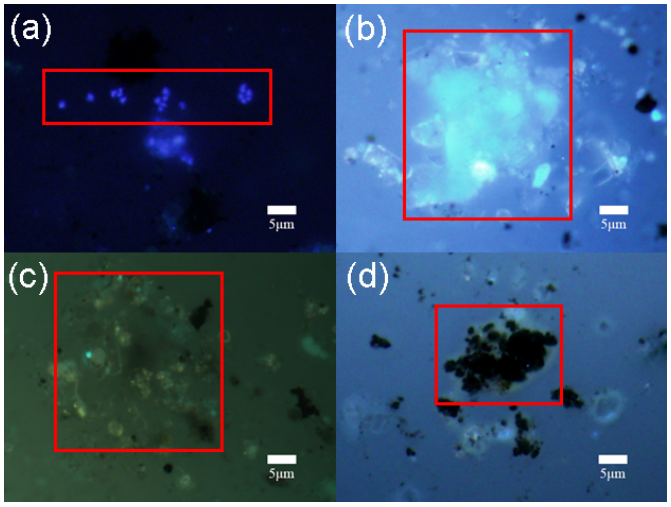

Fig. 5 Epifluorescence micrograph of (a) DAPI-stained bacteria (with diameters < 3 μm), (b) white particles (mineral particles), (c) yellow particles (organic matter) and (d) black particles (black carbon) in air samples. All photomicrographs were taken at a magnification of × 1000.

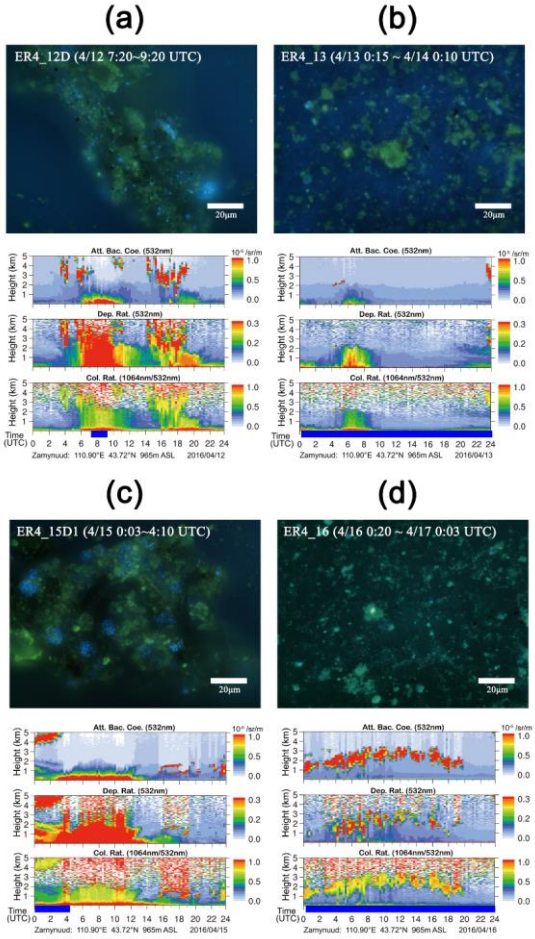

Fig. 6 Comparisons of bioaerosols collected during a dust event and a non-dust event (a and b) and during a dust event that transported dust over a long distance and a local dust event (c and d). Blue bars represent the periods over which samples were collected.

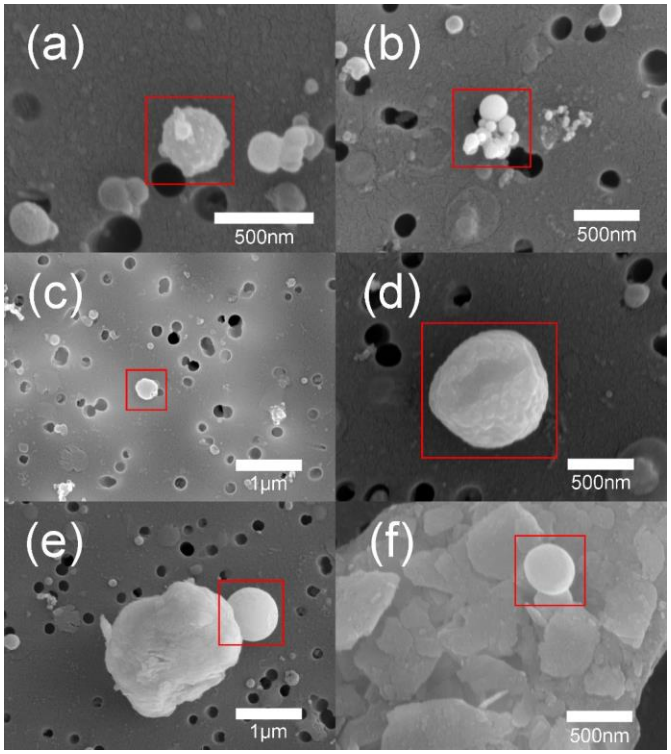

Fig. 7 State of bioaerosols under SEM. All of the pictures depict non-dust samples collected in Erenhot (panel a shows ER4_11N, whereas the others are from ER4_9).

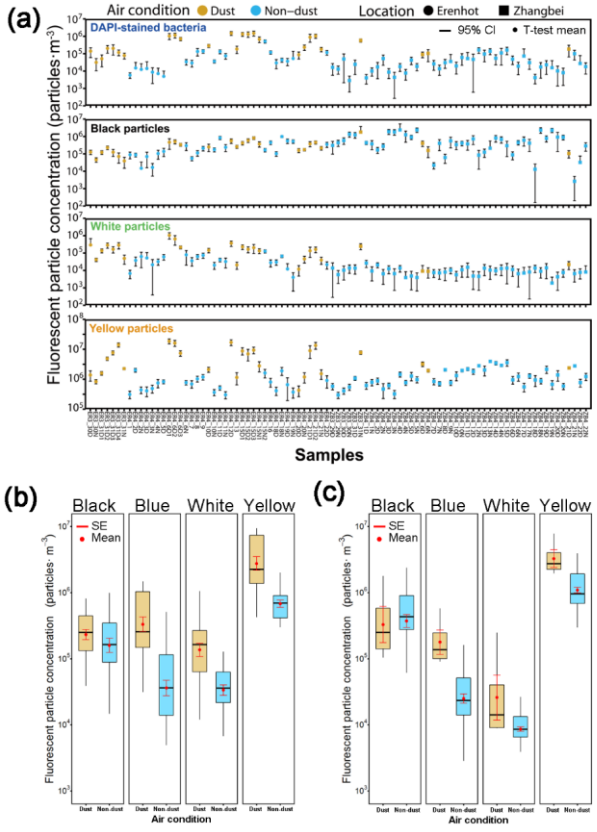

Fig. 8 Changes in the concentrations of fluorescent particles in the samples (a) and a comparison of the concentrations of fluorescent particles in the samples collected during dust events and non-dust events in Erenhot (b) and Zhangbei (c) (Black: black particles, Blue: DAPI-stained bacteria, White: white particles, Yellow: yellow particles, CI: confidence interval, SE: standard error).

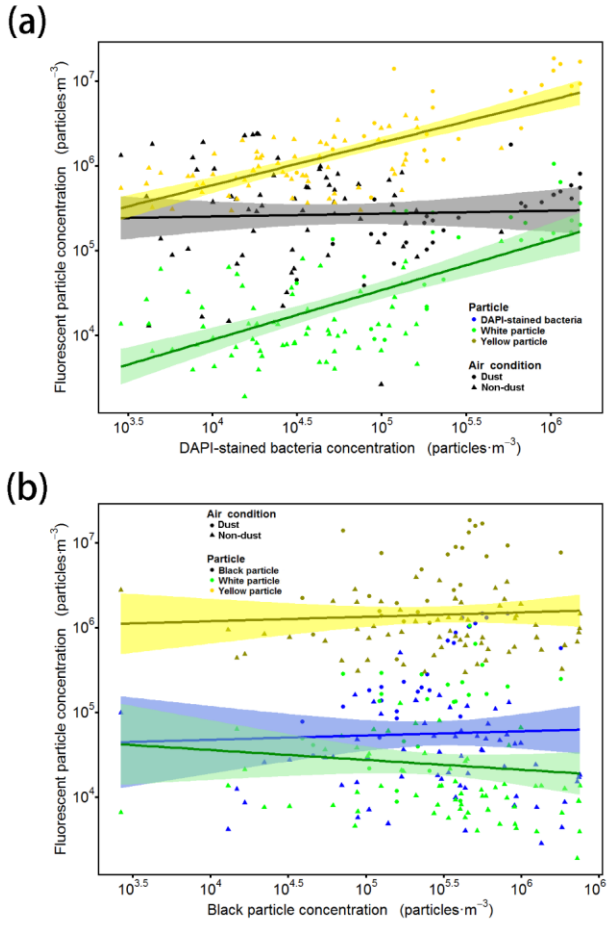
(a)
Fluorescent particle concentration (particles·m^{-3})
10^7
10^6
10^5
10^4
$10^{3.5}$
10^4
$10^{4.5}$
10^5
$10^{5.5}$
10^6
DAPI-stained bacteria concentration (particles·m^{-3})
Particle
DAPI-stained bacteria
White particle
Yellow particle
Air condition
Dust
Non-dust
(b)
Fluorescent particle concentration (particles·m^{-3})
Air condition
Dust
Non-dust
Particle
Black particle
White particle
Yellow particle
10^7
10^6
10^5
10^4
$10^{3.5}$
10^4
$10^{4.5}$
10^5
$10^{5.5}$
10^6
10^6
Black particle concentration (particles·m^{-3})

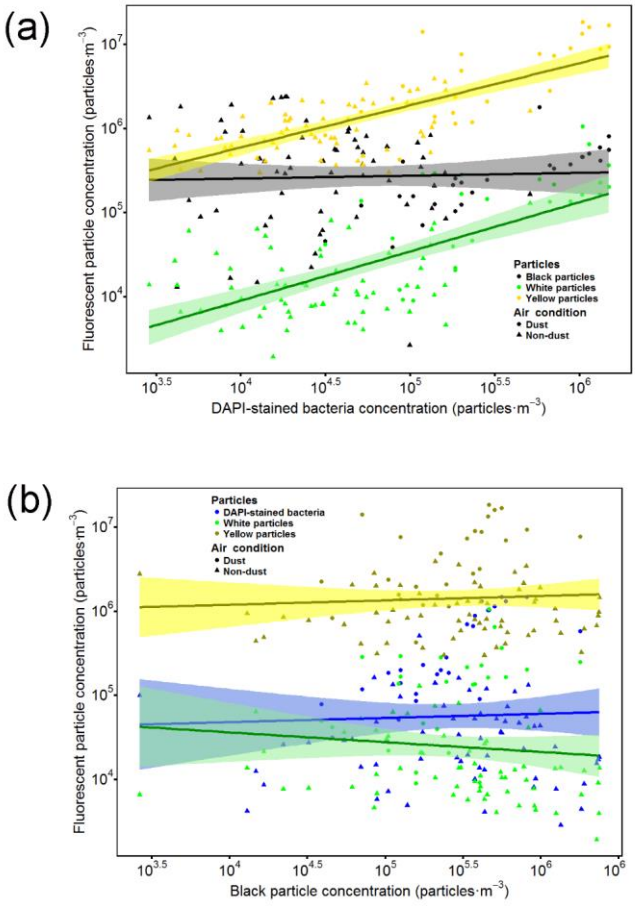

Fig. 9 Changes in the concentrations of the other three kinds of fluorescent particles with the concentrations of DAPI-stained bacteria (a) and the concentrations of black particles (b) in the dust and non-dust samples.

带格式的: 英语(英国)

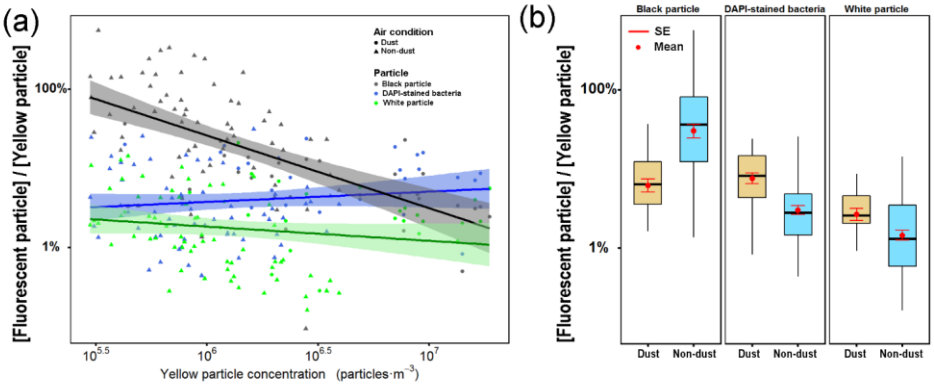

~~**Fig. 10 Ratios of the concentrations of three kinds of fluorescent particles to that of the yellow particles (a) and a comparison of these ratios in the dust and non-dust samples (b) (SE: standard error).**~~

Fig. 10 The concentration ratios of other three kinds of fluorescent particles to the yellow particles (a) and a comparison of these ratios in the dust and non-dust samples (b) (SE: standard error, y-axis is spaced logarithmically).

带格式的: 字体: (默认) Times New Roman, (中文) Times New Roman

带格式的: 字体: 10 磅

带格式的: 正文

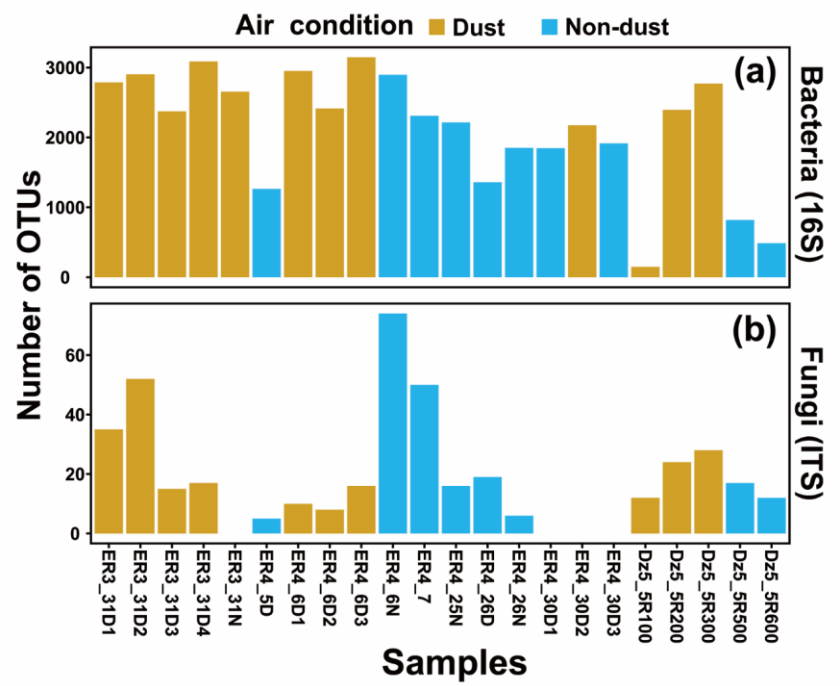

Fig. 11 Number of OTUs of bacteria (a) and fungi (b).

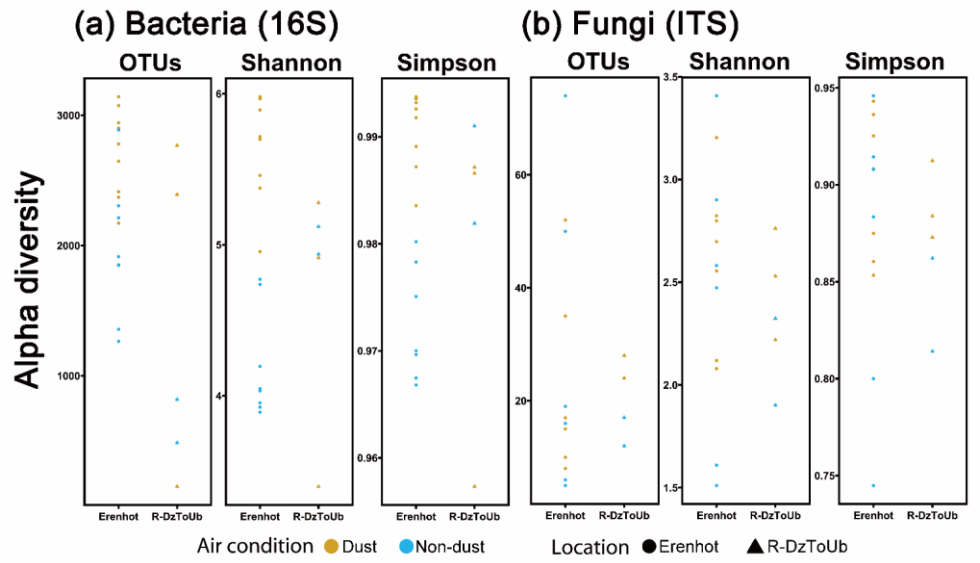

Fig. 12 Alpha diversity of bacteria (a) and fungi (b) (OTUs: Number of OTUs, Shannon: Shannon index, Simpson: Simpson index).

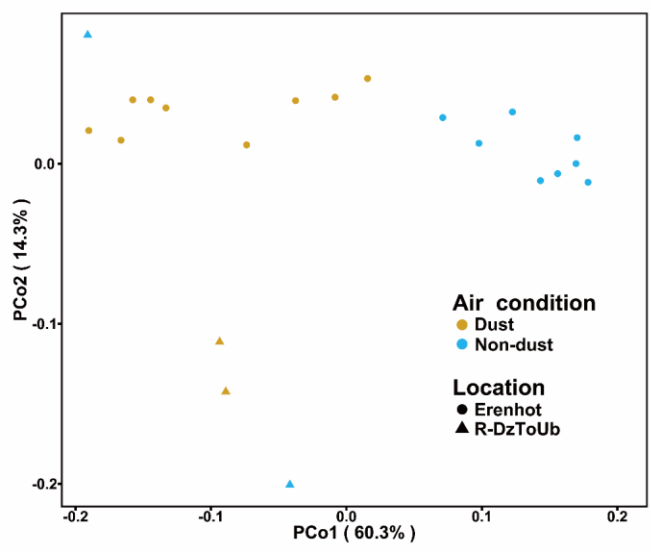

Fig. 13 Principal coordinates analysis of bacterial 16S rRDNA sequencing data obtained from 22 samples (PCo: principal coordinate).

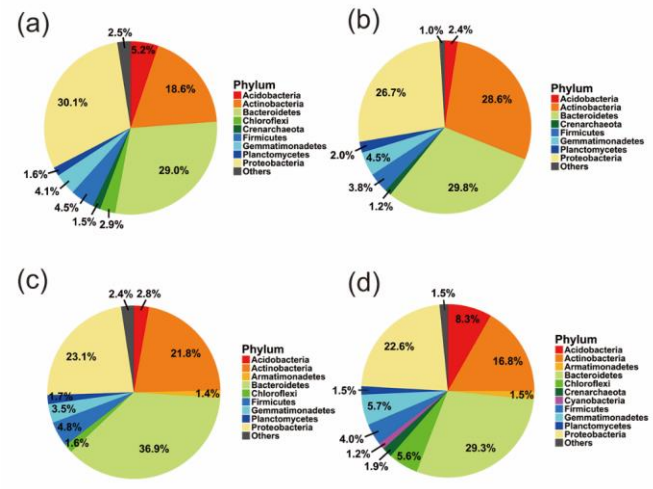

Fig. 14 Variations of the bacterial community composition at the phylum level (a) Dust samples of Erenhot, (b) Non-dust samples of Erenhot, (c) Dust samples of R-DzToUb and (d) Non-dust samples of R-DzToUb.

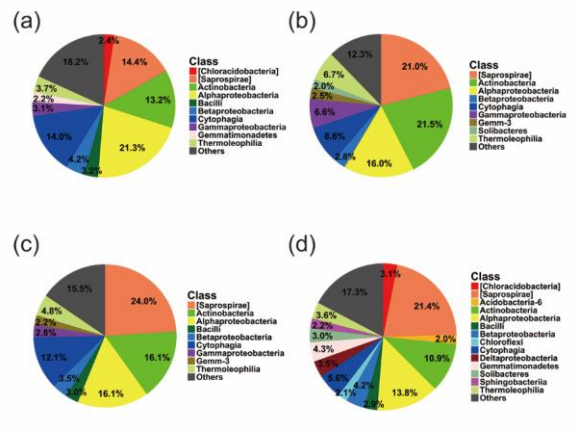

Fig. 15 Variations of the bacterial community composition at the class level (a) Dust samples of Erenhot, (b) Non-dust samples of Erenhot, (c) Dust samples of R-DzToUb and (d) Non-dust samples of R-DzToUb.

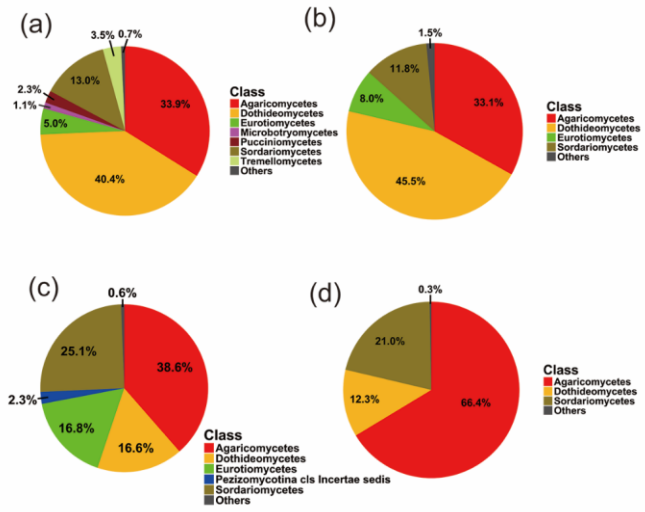

Fig. 16 Variations of the fungal community composition at the class level (a) Dust samples of Erenhot, (b) Non-dust samples of Erenhot, (c) Dust samples of R-DzToUb and (d) Non-dust samples of R-DzToUb.

Table S1 Sampling information of Erenhot.

Sample name	Start Time (UTC+8)	End Time (UTC+8)	Air condition	Time (min)	Volume (L)
ER3_30D	2016/3/30 8:40	2016/3/30 18:05	Dust	565	169.5
ER3_30N	2016/3/30 18:15	2016/3/31 8:15	Dust	840	252
ER3_31D1	2016/3/31 8:25	2016/3/31 13:25	Dust	300	90
ER3_31D2	2016/3/31 13:30	2016/3/31 15:30	Dust	120	36
ER3_31D3	2016/3/31 15:35	2016/3/31 17:30	Dust	115	34.5
ER3_31D4	2016/3/31 17:35	2016/3/31 19:37	Dust	122	36.6
ER3_31N	2016/3/31 21:45	2016/4/1 8:25	Dust	640	192
ER4_1	2016/4/1 8:40	2016/4/2 8:15	Non-dust	1415	424.5
ER4_2D	2016/4/2 8:23	2016/4/2 18:00	Non-dust	577	173.1
ER4_2N	2016/4/2 18:07	2016/4/3 8:14	Non-dust	847	254.1
ER4_3D	2016/4/3 8:20	2016/4/3 18:05	Non-dust	585	175.5
ER4_3N	2016/4/3 18:30	2016/4/4 17:40	Non-dust	1390	417
ER4_4N	2016/4/4 17:45	2016/4/5 8:17	Non-dust	872	261.6
ER4_5D	2016/4/5 8:20	2016/4/5 18:05	Non-dust	585	175.5
ER4_6D1	2016/4/6 8:15	2016/4/6 10:35	Dust	140	42
ER4_6D2	2016/4/6 10:45	2016/4/6 13:35	Dust	170	51
ER4_6D3	2016/4/6 13:45	2016/4/6 18:15	Dust	270	81
ER4_6N	2016/4/6 18:20	2016/4/7 8:25	Non-dust	845	253.5
ER4_7	2016/4/7 8:28	2016/4/8 8:15	Non-dust	1427	428.1
ER4_8	2016/4/8 8:20	2016/4/9 8:15	Non-dust	1435	430.5
ER4_9	2016/4/9 8:20	2016/4/10 8:15	Non-dust	1435	430.5
ER4_10D	2016/4/10 8:20	2016/4/10 18:40	Dust	620	186
ER4_10N	2016/4/10 18:45	2016/4/11 8:10	Non-dust	805	241.5
ER4_11D	2016/4/11 8:15	2016/4/11 18:10	Non-dust	595	178.5
ER4_11N	2016/4/11 18:15	2016/4/12 8:10	Non-dust	835	250.5
ER4_12D	2016/4/12 15:20	2016/4/12 17:20	Dust	120	36
ER4_13	2016/4/13 8:15	2016/4/14 8:10	Dust	1435	430.5
ER4_15D1	2016/4/15 8:03	2016/4/15 12:10	Dust	247	74.1
ER4_15D2	2016/4/15 12:15	2016/4/15 15:00	Dust	165	49.5
ER4_15D3	2016/4/15 15:10	2016/4/15 18:07	Dust	177	53.1
ER4_15N1	2016/4/15 18:12	2016/4/15 21:00	Dust	168	50.4
ER4_15N2	2016/4/15 21:05	2016/4/16 8:15	Non-dust	670	201
ER4_16	2016/4/16 8:20	2016/4/17 8:03	Non-dust	1423	426.9
ER4_18D	2016/4/18 8:00	2016/4/18 18:00	Non-dust	600	180
ER4_18N	2016/4/18 19:00	2016/4/19 8:50	Non-dust	830	249
ER4_19D	2016/4/19 8:55	2016/4/19 18:05	Non-dust	550	165
ER4_19N	2016/4/19 18:10	2016/4/20 8:00	Non-dust	830	249

ER4_20D	2016/4/20 8:05	2016/4/20 18:05	Dust	600	180
ER4_20N	2016/4/20 18:10	2016/4/21 12:00	Dust	1070	321
ER4_21D1	2016/4/21 12:10	2016/4/21 15:20	Dust	190	57
ER4_21D2	2016/4/21 16:00	2016/4/21 19:00	Dust	180	54
ER4_21N	2016/4/21 19:10	2016/4/22 9:00	Dust	830	249
ER4_22D	2016/4/22 9:05	2016/4/22 19:00	Non-dust	595	178.5
ER4_25N	2016/4/25 18:16	2016/4/26 7:35	Non-dust	799	239.7
ER4_26D	2016/4/26 8:05	2016/4/26 18:10	Non-dust	605	181.5
ER4_26N	2016/4/26 19:24	2016/4/27 7:12	Non-dust	708	212.4
ER4_30D1	2016/4/30 8:25	2016/4/30 12:01	Non-dust	216	64.8
ER4_30D2	2016/4/30 12:50	2016/4/30 15:54	Dust	184	55.2
ER4_30D3	2016/4/30 17:00	2016/4/30 20:11	Non-dust	191	57.3

Table S2 Sampling information of Zhangbei.

Sample name	Start Time (UTC+8)	End Time (UTC+8)	Air condition	Time (min)	Volume (L)
ZB3_29D	2016/3/29 6:58	2016/3/29 18:00	Non-dust	662	198.6
ZB3_29N	2016/3/29 18:36	2016/3/30 7:00	Non-dust	744	223.2
ZB3_30D	2016/3/30 7:27	2016/3/30 18:13	Non-dust	646	193.8
ZB3_30N	2016/3/30 19:00	2016/3/31 6:38	Non-dust	698	209.4
ZB3_31D	2016/3/31 7:15	2016/3/31 18:30	Non-dust	675	202.5
ZB3_31N	2016/3/31 18:40	2016/3/31 21:28	Dust	168	50.4
ZB4_1D	2016/4/1 7:02	2016/4/1 18:31	Non-dust	689	206.7
ZB4_1N	2016/4/1 18:38	2016/4/2 6:36	Non-dust	718	215.4
ZB4_2D	2016/4/2 6:45	2016/4/2 18:15	Non-dust	690	207
ZB4_2N	2016/4/2 18:21	2016/4/3 6:40	Non-dust	739	221.7
ZB4_3D	2016/4/3 6:49	2016/4/3 18:12	Non-dust	683	204.9
ZB4_3N	2016/4/3 18:26	2016/4/4 6:34	Non-dust	728	218.4
ZB4_4D	2016/4/4 6:41	2016/4/4 18:22	Non-dust	701	210.3
ZB4_4N	2016/4/4 18:28	2016/4/5 6:42	Non-dust	734	220.2
ZB4_5D	2016/4/5 6:50	2016/4/5 18:22	Non-dust	692	207.6
ZB4_5N	2016/4/5 18:31	2016/4/6 6:40	Non-dust	729	218.7
ZB4_6D	2016/4/6 6:50	2016/4/6 15:33	Dust	523	156.9
ZB4_6N	2016/4/6 15:41	2016/4/7 6:51	Dust	910	273
ZB4_7D	2016/4/7 6:57	2016/4/7 18:30	Non-dust	693	207.9
ZB4_7N	2016/4/7 18:36	2016/4/8 6:44	Non-dust	728	218.4
ZB4_8D	2016/4/8 6:50	2016/4/8 18:43	Non-dust	713	213.9
ZB4_9N	2016/4/9 18:24	2016/4/10 6:43	Non-dust	739	221.7
ZB4_10D	2016/4/10 6:50	2016/4/10 18:05	Non-dust	675	202.5
ZB4_10N	2016/4/10 18:11	2016/4/11 6:31	Non-dust	740	222

ZB4_11D	2016/4/11 6:40	2016/4/11 18:08	Non-dust	688	206.4
ZB4_12D	2016/4/12 8:34	2016/4/12 18:30	Non-dust	596	178.8
ZB4_12N	2016/4/12 18:40	2016/4/13 6:50	Non-dust	730	219
ZB4_13D	2016/4/13 6:58	2016/4/13 18:16	Non-dust	678	203.4
ZB4_13N	2016/4/13 18:26	2016/4/14 6:40	Non-dust	734	220.2
ZB4_14D	2016/4/14 6:51	2016/4/14 18:15	Non-dust	684	205.2
ZB4_14N	2016/4/14 18:24	2016/4/15 6:45	Non-dust	741	222.3
ZB4_15D	2016/4/15 6:53	2016/4/15 15:07	Non-dust	494	148.2
ZB4_16D	2016/4/16 7:07	2016/4/16 18:20	Non-dust	673	201.9
ZB4_16N	2016/4/16 18:28	2016/4/17 6:42	Non-dust	734	220.2
ZB4_17D	2016/4/17 6:52	2016/4/17 18:06	Non-dust	674	202.2
ZB4_17N	2016/4/17 18:17	2016/4/18 6:56	Non-dust	759	227.7
ZB4_18D	2016/4/18 7:05	2016/4/18 18:12	Non-dust	667	200.1
ZB4_18N	2016/4/18 18:20	2016/4/19 6:41	Non-dust	741	222.3
ZB4_19D	2016/4/19 6:52	2016/4/19 17:36	Non-dust	644	193.2
ZB4_19N	2016/4/19 18:29	2016/4/20 7:00	Non-dust	751	225.3
ZB4_20D	2016/4/20 7:10	2016/4/20 18:15	Non-dust	665	199.5
ZB4_20N	2016/4/20 18:25	2016/4/21 6:50	Non-dust	745	223.5
ZB4_21D	2016/4/21 7:00	2016/4/21 18:19	Dust	679	203.7
ZB4_21N	2016/4/21 18:47	2016/4/22 6:53	Non-dust	726	217.8
ZB4_22D	2016/4/22 7:50	2016/4/22 18:02	Non-dust	612	183.6
ZB4_22N	2016/4/22 19:03	2016/4/23 6:47	Non-dust	704	211.2

Table S3 Sampling information of R-DzToUb

Sample name	Sampling time (UTC+8)	Air condition	Time (min)	Volume (L)	Location
Dz5_5R100	2016/5/5 9:25 − 10:25	Dust	60	30	0km to 100km from Daranzadgad
Dz5_5R200	2016/5/5 10:56 − 11:56	Dust	60	30	100km to 200km from Daranzadgad
Dz5_5R300	2016/5/5 12:21 − 13:21	Dust	60	30	200km to 300km from Daranzadgad
Dz5_5R500	2016/5/5 15:43 − 16:43	Non-dust	60	30	300km to 400km from Daranzadgad
Dz5_5R600	2016/5/5 17:05 − 18:05	Non-dust	60	30	500km to 600km from Daranzadgad

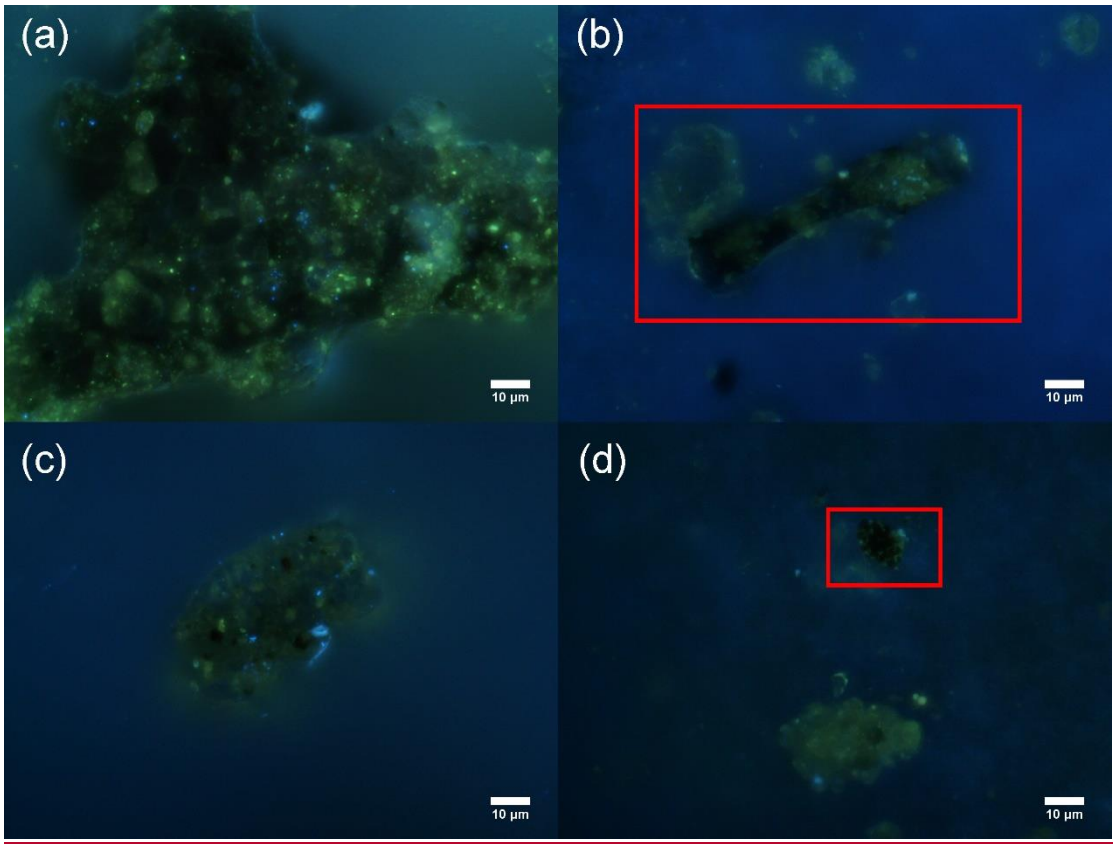

Fig. S4 Epifluorescence micrograph of mixed-type aerosols, (a) from the sample ER4_15D2, (b) and (d) from the sample ER4_11N, (c) from the sample ER4_15N1.

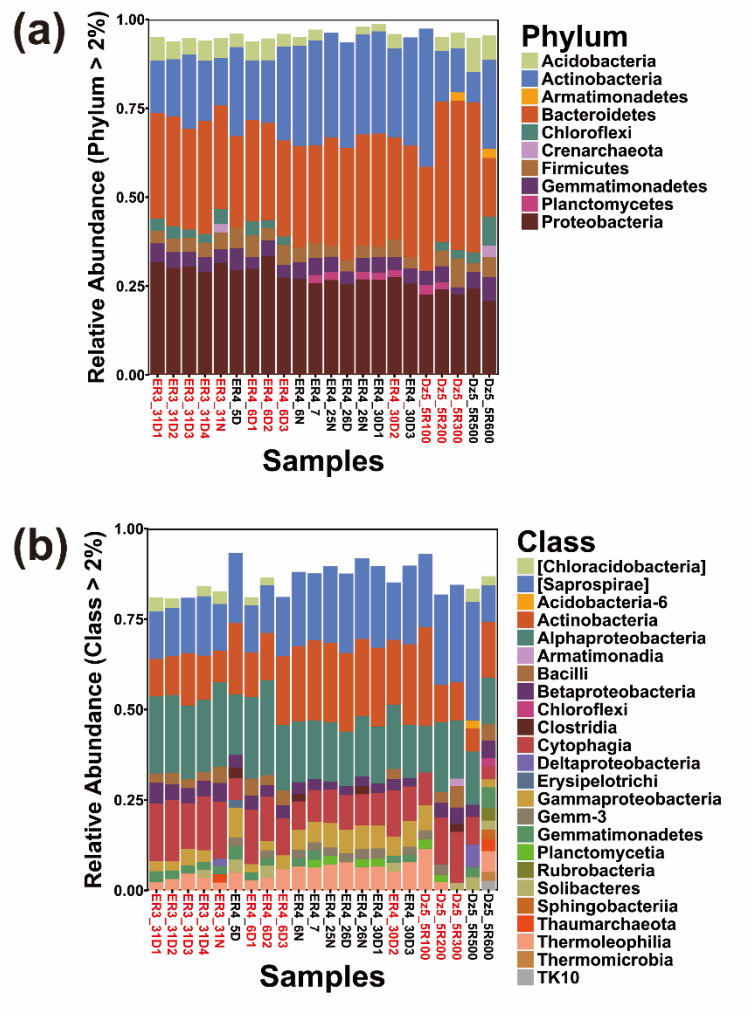

Fig. ~~S4~~ S5 Variations of the bacterial community composition at (a) the phylum level and (b) the class level in the dust (red font) and non-dust samples (black font).

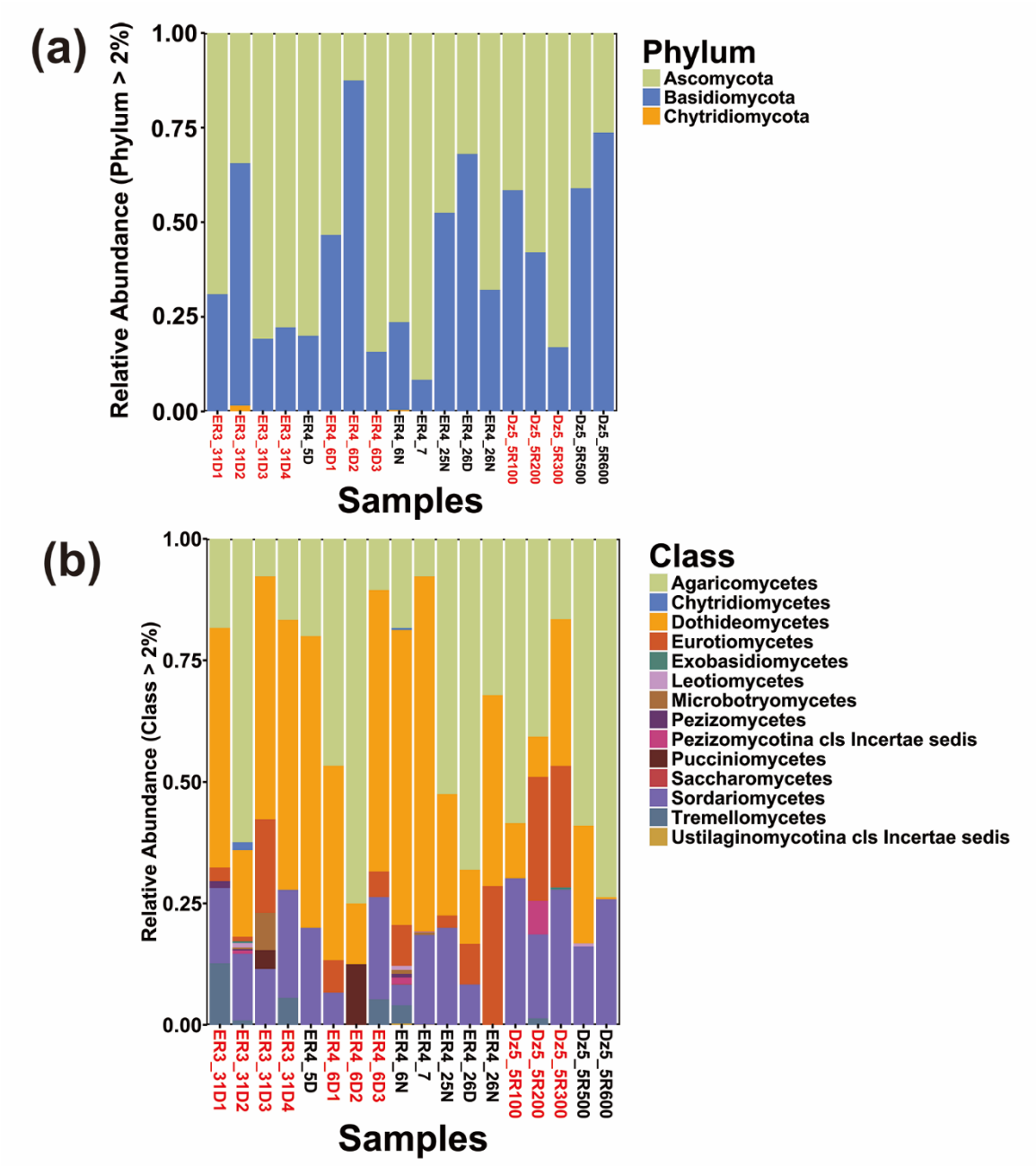

Fig. ~~S5~~ S6 Variations of the fungal community composition at (a) the phylum level and (b) the class level in the dust (red font) and non-dust samples (black font).